PHYLOGEOGRAPHIC ASSESSMENT OF THE HEERMANN’S KANGAROO RAT

A Thesis

by

BRIDGETT BENEDICT DOWNS

Submitted to the Office of Graduate and Professional Studies of
Texas A&M University
in partial fulfillment of the requirements for the degree of

MASTER OF SCIENCE

Chair of Committee,	Jessica E. Light
Committee Members,	Thomas E. Lacher
	William J. Murphy
Head of Department,	David Caldwell

August 2018

Major Subject: Wildlife and Fisheries Sciences

ABSTRACT

Heermann's kangaroo rats (*Dipodomys heermanni*; Rodentia: Heteromyidae) are endemic to California and primarily found in the dry, gravelly grassland and open chaparral habitats of the San Joaquin Valley. Current taxonomy (based on morphology and habitat use) recognizes nine subspecies within this kangaroo rat species. Management practices of *D. heermanni* primarily are based on this classification, but this taxonomy may not accurately reflect unique lineages in need of conservation.

Using molecular and morphological data, I performed a phylogeographic assessment of *D. heermanni* examining relationships within and among the nine subspecies across the full geographic range of the species. Phylogenetic and network analyses of mitochondrial data from over 90 museum specimens (representing all nine subspecies distributed across the range of the species) revealed no substantial genetic differentiation within *D. heermanni*. Similarly, a geometric morphometric analysis of the cranium of over 200 adult *D. heermanni* museum specimens (again representing all subspecies across the geographic distribution of species) resulted in no apparent morphological clustering across geography. My analyses indicate that recognition of all nine subspecies is likely unwarranted and that conservation and management practices *of D. heermanni* are in need of revision.

DEDICATION

I dedicate this thesis to my parents, Jennifer and Dr. Howard Benedict, and to my husband, Christopher Downs, for their love and support.

ACKNOWLEDGEMENTS

I would like to thank my committee: Dr. Jessica E. Light, Dr. Thomas Lacher, and Dr. William Murphy; my lab mates; and my husband for their guidance and support throughout the course of this research.

CONTRIBUTORS AND FUNDING SOURCES

This work was supervised by a thesis committee consisting of Drs. Jessica E. Light and Thomas E. Lacher of the Department of Wildlife and Fisheries Sciences and Dr. William J. Murphy of the Department of Veterinary Integrative Biosciences.

This work would not be possible without the help of the generous staff and curators, and loans from the Museum of Vertebrate Zoology at Berkeley, The Natural History Museum of Los Angeles County, and Louisiana State University Museum of Natural Science. It would also not be possible without the guidance of Adrian Castellanos in morphological methodology and analysis. I would also like to thank collaborators Joseph DiDonato and Dr. Douglas Bell for their assistance and advice. Lastly, I thank Dr. James Patton for sharing his cytochrome-b data and providing advice regarding project design. All other work conducted for the thesis was completed by the student independently.

Graduate study was supported by a $1,500 grant from Fletcher Conservation Bank, a $1,000 Will Roach Scholarship and a $1,000 Richard Baldouf Scholarship both from the Department of Wildlife and Fisheries Sciences at Texas A&M University, and a $750 Graduate Student Research and Presentation Grant from the Association of Former Students and the Office of Graduate and Professional Studies at Texas A&M University.

TABLE OF CONTENTS

LIST OF FIGURES

LIST OF TABLES

INTRODUCTION

In mammalogy, use of modern molecular and morphological techniques can result in taxonomic recommendations that differ from the original taxonomic designations, oftentimes resulting in discussions of species and subspecies concepts (e.g., Wilson and Brown 1953; Lidicker 1962; Stanford 2001; Gippoliti and Amori 2007; Ruiz-García et al. 2014; Sackett et al. 2014; Malaney et al. 2017; Patton and Conroy 2017). In the case of subspecies concepts, discussions have transitioned from holding subspecies to the rigorous guidelines created for species, to defining subspecies by geographic boundaries separating lineages, to contesting the value of subspecies (e.g., Wilson and Brown 1953; Lidicker 1962; Braby et al. 2012; Patton and Conroy 2017). Lidicker (1962) defined a subspecies as "[…] a relatively homogeneous and genetically distinct portion of a species which represents a separately evolving, or recently evolved, lineage with its own evolutionary tendencies, inhabits a definite geographical area, is usually at least partially isolated, and may intergrade gradually, although over a fairly narrow zone, with adjacent subspecies." Lidicker (1962) further describes subspecies as "populations which have made initial steps in the direction of species formation", and emphasizes that in our search for elucidating subspecies relationships and our desire to preserve species from degradation, it is inevitable that a search for differentiation (molecular and/or morphological) will be performed (Lidicker 1962). While definitions of subspecies abound in the literature, most emphasize genetic and morphological distinctness as well as geographic isolation (e.g., Wilson and Brown 1953; Lidicker 1962; Braby et al. 2012; Patton and Conroy 2017). An overarching goal of determining subspecific designations is to accurately reflect probable distinct groups within a species, some of which may be in need of protection (Braby et al. 2012; Patton and

Conroy 2017). This is especially a concern for understudied, geographically widespread species such as the Heermann's kangaroo rat (*Dipodomys heermanni*; Rodentia: Heteromyidae).

Dipodomys heermanni is a nocturnal rodent that is primarily found in the San Joaquin Valley of California (Fig. 1) occupying dry, gravelly grasslands and open chaparral habitats (Grinnell 1922; Kelt 1988). Similar to other kangaroo rats, the diet of *D. heermanni* consists primarily of seeds and, as such, this species plays a key role in seed dispersal (Kelt 1988). Additionally, kangaroo rats prefer areas with loose soil where they build and occupy burrows for shelter and seed storage (Kelt 1988). These burrows, and their granivorous lifestyle, can often change the vegetation structure of their habitats (Cosentino et al. 2014). Thus, this species plays an important and vital role in its ecosystem (Hudson 1958).

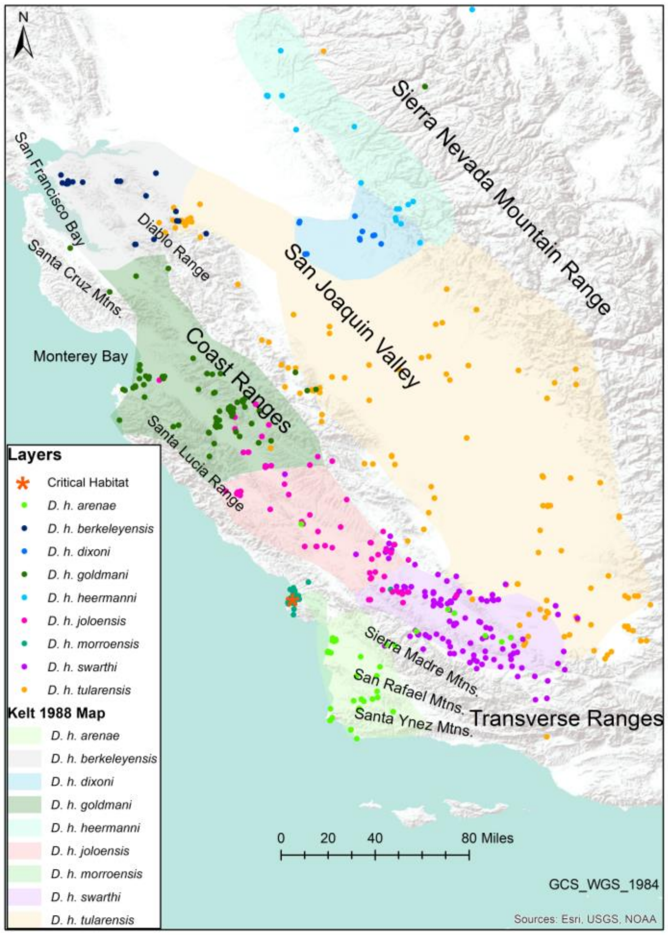

Figure 1. Distribution of *Dipodomys heermanni* across California. *Dipodomys heermanni* subspecies localities downloaded from VertNet are indicated by filled circles and are overlain on Kelt's (1988) subspecific distribution map (shaded regions). Critical habitat for *D. h. morroensis* is indicated with a red star and biogeographic regions are noted.

The name *Dipodomys heermanni* was first given to the species by Le Conte in 1853, and there have been many revisions to the species since (Le Conte 1853; Hall 1981; Kelt 1988). *Dipodomys californicus* (Grinnell 1922), *D. eximus* (Grinnell 1922), and *D. saxatilis* (Grinnell and Linsdale 1929) were regarded as subspecies of *D. heermanni*, but are now synonymous to *D.*

californicus due to morphological (four toes on their hind foot; *D. heermanni* has five toes), chromosomal, and biochemical data (Johnson and Selander 1971; Fashing 1973; Stock 1974; Patton et al. 1976; Hall 1981; Wilson and Reeder 2005). Nine subspecies are currently recognized within *D. heermanni* (Fig. 1; Grinnell 1922; Boulware 1943; Patton et al. 1976; Hall 1981; Kelt 1988). The majority of these subspecies were originally recognized as full species within *Dipodomys* or *Perodipus* (a synonym of *Dipodomys*), including *D. h. berkeleyensis*, *D. h. dixoni*, *D. h. goldmani*, *D. h. heermanni*, *D. h. jolonensis*, *D. h. morroensis*, and *D. h. swarthi* (Le Conte 1853; Merriam 1894, 1904, 1907; Grinnell 1919a; b, 1922; Boulware 1943; Hall 1981; Kelt 1988). *Dipodomys h. tularensis* was once recognized as a subspecies of *Dipodomys [Perodipus] agilis* (Merriam 1904) and *D. h. arenae* was recently designated a subspecies (Boulware 1943; Hall 1981).

Seven of the nine currently recognized *D. heermanni* subspecies (*D. h. berkeleyensis*, *D. h. dixoni*, *D. h. goldmani*, *D. h. heermanni*, *D. h. jolonensis*, *D. h. swarthi*, and *D. h. tularensis*) have maintained their names as described by Grinnell in 1922. Grinnell (1922) separated these subspecies and *D. morroensis* (now *D. h. morroensis*) from each other based on general geographic locations (Fig. 1), coat color and characteristics, breadth of the skull, rostrum length and width, and ear size (Table 1). Notably, Grinnell (1922) did not perform any statistical analyses to morphologically differentiate subspecies, sometimes examining as few as four specimens per subspecies. The most recent addition to *D. heermanni* was *D. h. arenae* by Boulware (1943) after an examination of 29 *D. h. arenae* specimens. Boulware (1943) described *D. h. arenae* as being darker, having heavier and blacker facial crests, darker tail tufts, smaller hind feet, and smaller auditory bullae than *D. h. jolonensis* and *D. h. swarthi*, a wider supraoccipital than *D. h. jolonensis*, and shorter upper incisors than *D. h. swarthi*. Boulware's

(1943) study of *D. h. arenae* also prompted the reclassification of *D. morroensis* to *D. h. morroensis* because the characteristics of *D. h. arenae* were intermediate between *D. morroensis* and *D. h. jolonensis* and *D. h. swarthi*, with *D. h. morroensis* being the darkest and having the most intense markings and *D. h. swarthi* being the lightest (Boulware 1943). Boulware (1943) described the skull of *D. h. arenae* to be intermediate in size, degree of bullae inflation, width of supraoccipital, and length of nasals between *D. h. morroensis* and *D. h. jolonensis* and *D. h. swarthi* (Boulware 1943).

Table 1. Characters used in Grinnell (1922) to characterize adult *Dipodomys heermanni* subspecies.

Current Subpecies Name	**Coat Color**	**Skull Characteristics**	**Other Characteristics**	**Number of Specimens Examined**
D. h. berkeleyensis	dark; facial arietiform marking bold; dorsal dark black tail-stripe ≥ width lateral white stripe, white flank stripe, cinnamon-buff or darker dorsal body color, tail heavily crested, terminal hairs > 20 mm long	breadth of skull across bullae < 24.3mm, >23.6mm; length of nasals > 14mm		4
D. h. dixoni	dark; facial arietiform marking bold; dorsal dark black tail-stripe ≥ width lateral white stripe, white flank stripe, cinnamon-buff or darker dorsal body color	breadth of skull across bullae < 23.6mm; length of nasals < 14mm		18
D. h. goldmani	dark; facial arietiform marking bold; dorsal dark black tail-stripe ≥ width lateral white stripe, white flank stripe, cinnamon-buff or darker dorsal body color, weak tail crest, terminal hairs <20 mm long	breadth of skull across bullae < 25mm, >23.6mm; length of nasals > 14mm		174
D. h. heermanni	dark; facial arietiform marking bold; dorsal dark black tail-stripe ≥ width lateral white stripe, white flank stripe, cinnamon-buff or darker dorsal body color	breadth of skull across bullae < 25mm, >24.3mm; length of nasals > 14mm		61
D. h. jolonensis	dark; facial arietiform marking bold; dorsal dark tail-stripe ≥ width lateral white stripe and grizzled; white flank stripe; warm buff dorsal body color	breadth of skull across bullae > 25mm		93
D. h. morroensis	dark; facial arietiform marking bold; dorsal dark tail-stripe ≥ width lateral white stripe, white flank stripe incomplete or absent			61
D. h. swarthi	medium or pale; facial arietiform marking weak; dorsal dark tail-stripe ≤ width lateral white stripe; dorsum near ochraceous-buff	breadth of skull across bullae > 24.9mm	ears < 12mm height	36
D. h. tularensis	medium or pale; facial arietiform marking weak; dorsal dark tail-stripe ≤ width lateral white stripe; warm buff, pinkish buff or cinnamon-buff color	narrowest place between mastoid bullae < 2mm wide; rostrum near end < 4.1mm wide	ears > 12mm height	169

Other than the additions made by Boulware (1943), there has not been an addition of new morphological characteristics, or re-evaluation of the specific characters as described in Table 1 (Grinnell 1922). In general, morphology overlaps and intergrades among the *D. heermanni* subspecies (Table 1 and description of *D. h. arenae* above). Thus, the recognition of the nine *D. heermanni* subspecies is generally based on plastic morphological traits and geography (Fig. 1). A *Dipodomys* species distribution map (including five species and their respective subspecies) was created by Hall (1981) and modified by Kelt (1988) to show only *D. heermanni* subspecies (Fig. 1). The geographic breaks among subspecies are generally undetermined, although it has been suggested that *D. h. morroensis* is restricted to the sand dunes of Morro Bay (Kofron and Villablanca 2016).

Despite the lack of information regarding the geographic distribution of *D. heermanni* subspecies, several subspecies are of interest at the state and federal level and have been the topic of previous phylogenetic and phylogeographic research. For example, extensive research has been undertaken on the federally and state listed *D. h. morroensis* (Congdon and Roest 1975; Matocq and Villablanca 2001; Villablanca 2007; Kofron and Villablanca 2016). Prior genetic studies examining mitochondrial and microsatellite data obtained from *D. h. morroensis* specimens held in natural history collections support that *D. h. morroensis* is genetically distinct (reviewed in Kofron and Villablanca 2016). Genetic diversity in the mitochondrial data, however, was low, possibly the result of historical processes rather than a recent bottleneck (Matocq and Villablanca 2001). Notably, these previous studies compared *D. h. morroensis* to only a maximum of four other *D. heermanni* subspecies. To date, no genetic comparison, and limited morphological comparisons have been made between *D. h. morroensis* and all other *D. heermanni* subspecies. Similarly, multiple attempts to explore the distinctiveness of *D. h.*

berkeleyensis have been undertaken, but never published. *Dipodomys h. berkeleyensis* is presumed extinct, yet recognized as a special-status species in The U.S. Fish and Wildlife Service (USFWS) Draft Recovery Plan (2002) for chaparral and scrub community species east of San Francisco Bay (USFWS 2017). Most of the unpublished studies examining *D. h. berkeleyensis* have compared this subspecies to only one or two other subspecies.

To date, there has been no wide-scale phylogeographic examination of *D. heermanni* across its entire geographic range. However, there has been some examination of karyotypic variation among six of the currently recognized subspecies (Fashing 1973; Stock 1974; *D. h. berkeleyensis*, *D. h. dixoni*, and *D. h. heermanni* were not included), protein variation of *D. heermanni* relative to other *Dipodomys* species (Johnson and Selander 1971; Patton et al. 1976), and morphological variation within *D. heermanni* (Table 1; Grinnell 1922; Boulware 1943) and relative to other *Dipodomys* species (Grinnell 1922; Lidicker 1960; Risser 1976; Baumgardner and Kennedy 1994; Carrasco 2000). The most recent examinations of relationships among 20 *Dipodomys* species were performed within a greater context of all Heteromyidae (Alexander and Riddle 2005; Hafner et al. 2007). To date, no one has examined the validity of all nine *D. heermanni* subspecies based on molecular data, nor has anyone rigorously assessed morphological variation within the species. Without this context, it is unknown if any of the subspecies represent evolutionary distinct units (Moritz 1994).

Using molecular and morphological data, this study undertakes a much-needed taxonomic reassessment of *D. heermanni*, across its entire geographic range. In doing so, I will determine if recognition of all nine subspecies is valid and, if necessary, I will make taxonomic recommendations based on biogeographically-defined lineages within the species such that appropriate mechanisms can be put in place for conservation and management.

MATERIALS AND METHODS

All objectives of the proposed project were met solely using archival specimens stored in natural history museums (Appendix 1 and 2). Using VertNet (vertnet.org), I carefully screened data from over 3,000 *D. heermanni* specimens (29 January 2017) for appropriateness for my study (Fig. 1). Specifically, I looked for specimens that had a known (and unique) locality and a skin and/or skull for genetic and morphological work. In total, 97 and 209 specimens were obtained for molecular and morphological analyses, respectively (Appendix 1 and 2). Subspecific names of the specimens used were verified or determined by overlaying Kelt's (1988) range map over the localities of each specimen as recorded in VertNet (Fig. 2, Appendix 1 and 2).

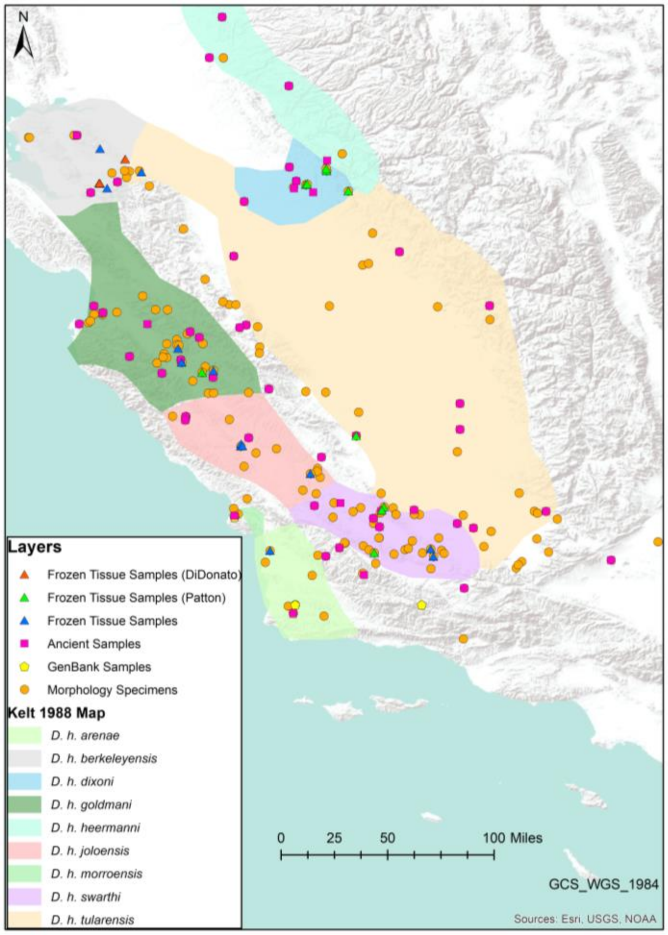

Figure 2. *Dipodomys heermanni* specimens analyzed in this study (colored shapes) overlain on Kelt's (1988) subspecific distribution map (shaded regions).

Molecular Laboratory Methods

Fresh tissue (from recently collected specimens) from 36 specimens and ancient tissues (toe pad clips and/or skull tissue from older specimens from which there are no tissues) from 61 specimens were obtained from museum collections for molecular analysis (Appendix 1). Fresh tissues were stored at -20°C, while toe pad clips and skull tissues were stored at room temperature until extraction.

DNA was extracted from fresh tissues using Omega Bio-Tek E.Z.N.A® Tissue DNA Kit (Omega Bio-Tek, Norcross, Georgia) according to manufacturer's recommendations. DNA from museum specimen toe pad clips and skull tissue was extracted in a dedicated ancient laboratory using a QIAmp DNA Micro Kit (QIAGEN Inc, Valencia, California) following manufacturer's instructions, including an additional 24 h presoak in a 1X phosphate-buffered saline buffer solution. For fresh tissue samples, the mitochondrial genes cytochrome-b (*Cytb*; 414 base pairs [bp]) and NADH dehydrogenase 2 (*ND2*; 981 bp), and the mitochondrial control region (*Dloop*; 363 bp) were amplified using primers MVZ04 and MVZ05 (Smith and Patton 1991), L5215ND2 and H6313ND2 (Sorenson et al. 1999), and L15926DIOR and H00651 (Kocher et al. 1989), respectively. Mitochondrial markers from ancient samples were amplified using newly designed *Cytb* primers (414 bp collectively; Appendix 3) and previously used *Dloop* primers (TAS-Dpd3, Dpd4-Dpd7, Dpd6-TDKD; 363 bp collectively; Thomas et al. 1990; Villablanca 1994; Matocq and Villablanca 2001). All PCRs were performed in 25 µl reaction volumes using 10 µl of EmeraldAmp Max PCR Master Mix (Thermo Fisher Scientific, Waltham, Massachusetts), 1 µl of each primer (at 10mM), and 1 µl of DNA template. Polymerase chain reaction cycling parameters for each gene fragment differed slightly depending on the sample (fresh or ancient) and gene. For fresh tissues, *Cytb* required an initial denaturation at 95°C for 5min, followed by 35 cycles at 95°C (30s), 52°C (60s), and 72°C (90s), and a final extension of 72°C for 5 min. *ND2* required an initial denaturation at 94°C for 5min, followed by 40 cycles at 94°C (30s), 50°C (30s), and 72°C (90s), and a final extension of 72°C for 5 min. Lastly, *Dloop* required an initial denaturation at 94°C for 5min, followed by 35 cycles at 94°C (30s), 56°C (30s), and 72°C (90s), and a final extension of 72°C for 5 min. *Cytb* ancient samples followed the same protocol as for the fresh samples, but included an additional five cycles. Parameters for ancient *Dloop* samples were as described in Matocq and Villablanca (2001). *ND2* was not amplified in the ancient lab. If fragments failed to amplify, annealing temperatures were adjusted accordingly. All amplified fragments were purified using ExoSAP-IT (USB Corporation, Cleveland, Ohio), and all sequencing reactions were performed at DNA Analysis Facility on Science Hill at Yale University using ABI Prism BigDye Terminator cycle sequencing protocols (New Haven, CT) and the same primers as those used for PCR. Sequencher 4.10.1 (GeneCodes Corporation, Ann Arbor, Michigan) was used to edit the sequences and Se-Al version 2.01a11 (Rambaut 1996) was used to align the sequences by eye for each gene and to trim off primer regions and excess 3' and 5' bases to result in maximum overlap among individuals. All sequences were submitted to GenBank (Appendix 1). An additional 17 *Cytb* sequences were shared with us by Dr. James Patton and 34 *Dloop* sequences were downloaded from GenBank (Appendix 1).

Molecular Analysis

Phylogenetic analyses were performed for fresh tissue samples for *Cytb* (including additional data provided by Dr. James Patton), *ND2,* and *Dloop* (including additional data downloaded from GenBank) individually and concatenated, including appropriate outgroup taxa downloaded from GenBank (Appendix 1). *Cytb* and *Dloop* fresh tissue datasets were also combined with the ancient samples and analyses were performed on the genes individually and in a concatenated framework. In total, seven datasets were analyzed: fresh tissue 1) *Cytb*, 2) *ND2*, 3) *Dloop*, and 4) *Cytb, ND2,* and *Dloop* concatenated, and ancient and fresh tissue 5) *Cytb*, 6) *Dloop*, and 7) *Cytb* and *Dloop* concatenated.

Prior to phylogenetic analyses, PartitionFinder (Lanfear et al. 2012) or jModelTest (for *Dloop* only; Posada 2008) was used to identify the best partitions and models of molecular evolution for each partition across each dataset (Appendix 4). Using these partitions and models of evolution, individual genes were analyzed separately as well as in a combined framework in MrBayes v.3.2.6 (Ronquist and Huelsenbeack 2003) via the CIPRES Science Gateway (Miller et al. 2010). Analyses were run with random starting trees, 10 million generation runs with four incrementally heated chains (Metropolis-coupled Markov chain Monte-Carlo- Ronquist and Huelsenbeack 2003), and sampled at intervals of 1,000 generations. Two runs were conducted simultaneously and independently, and 25% of the sampled trees were disregarded at burn-in. To test for subspecies monophyly, Bayesian phylogenetic constraint analyses also were performed using a stepping-stone sampling method (Xie et al. 2011), and evaluated using Bayes factors in MrBayes following Bergsten et al. (2013).Constraint analyses were only performed on the fresh and ancient *Cytb* and *Dloop* datasets.

A statistical parsimony analysis (Templeton et al. 1992) using the TCS function in Popart (Leigh and Bryant 2015) was performed to construct haplotype networks for five datasets (concatenated datasets were excluded). TCS assembles the most parsimonious haplotype tree (with linkages between taxa representing mutational events) and estimates a 95% plausible set for all haplotype connections. Genetic divergences within and among phylogenetic lineages were assessed using PAUP* (Swofford 2003).

Morphological Methods

Dorsal and ventral views of the cranium of 209 adult specimens of *D. heermanni* (five of which were type specimens) were photographed for two-dimensional morphological analysis (Appendix 2). Twenty landmarks and 60 semilandmarks were placed on the dorsal view and 34 landmarks and 60 semilandmarks were placed on the ventral view for each specimen used (Figs. 3 and 4, respectively). All landmarks were selected with careful consideration to include characters used in the original description of the species and capture known dental variation within *Dipodomys* (e.g., Grinnell 1922; Boulware 1943; Carrasco 2000). For example, the 60 semilandmarks for both dorsal and ventral views were used to represent the tympanic bulla, a region of the skull highlighted in previous morphological assessments (Grinnell 1922; Boulware 1943). Landmarks were digitalized using tpsUtil32 and tpsDig232 software (Rohlf 2015).

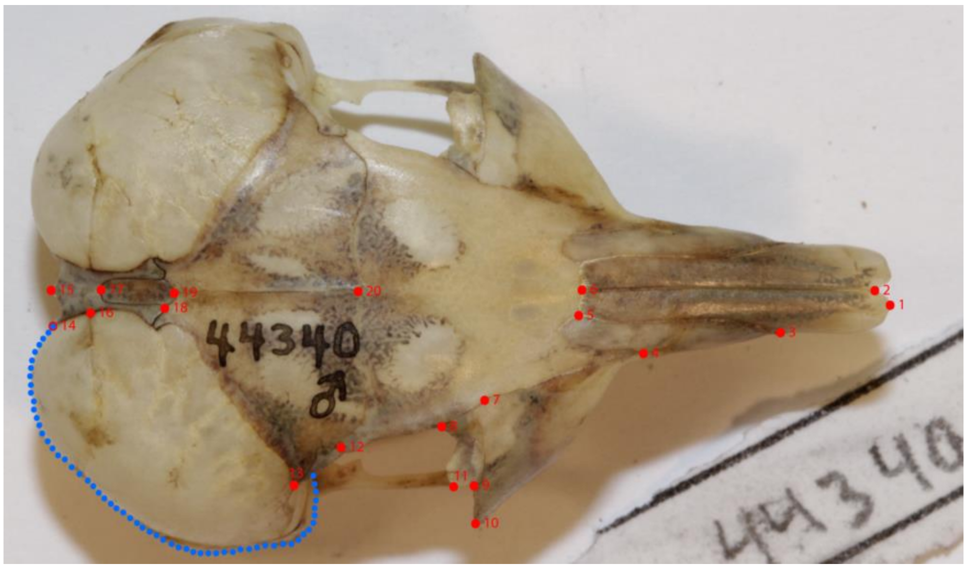

Figure 3. Dorsal landmark scheme for *Dipodomys heermanni* morphological analysis, including 20 landmarks (red dots) and 60 semilandmarks (blue dots).

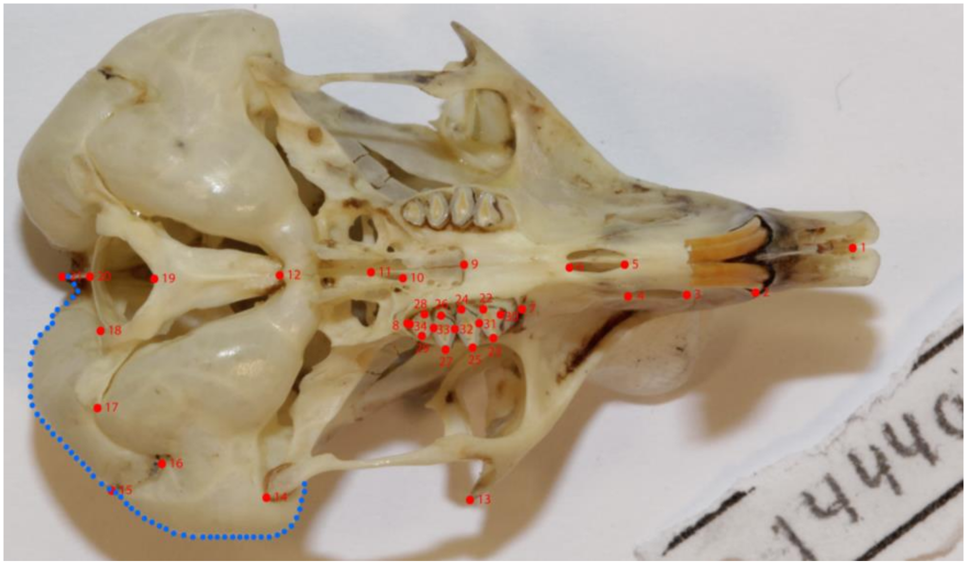

Figure 4. Ventral landmark scheme for *Dipodomys heermanni* morphological analysis, including 34 landmarks (red dots) and 60 semilandmarks (blue dots).

Morphological Analysis

All statistical analyses were conducted in R statistical software version 3.4.3 (Team 2017). Morphological analyses were conducted separately for the dorsal and ventral views of the skull. For both views, a generalized Procrustes transformation was used to obtain centroid size, normalize the orientation and size of the shape, and to slide semilandmarks along their tangent directions using the packages geomorph (Adams et al. 2017) and shapes (Lawing and Polly 2010; Dryden 2017). A principal component analysis (PCA) was then performed using the Procrustes transformed landmark data to create shape variables used in further analyses. Due to the preponderance of landmarks and semilandmarks used, analyses were only conducted on the axes comprising 95% of the variation.

A Welch two sample t-test on shape variables was used to test sexual dimorphism in shape. Mclust, a hierarchical model-based clustering algorithm (Fraley et al. 2012), was used to determine the number of distinct morphological groups given the shape variables (Scrucca et al. 2016). Mclust fits the data using Gaussian models into various clusters and identifies the most appropriate clustering and classification scheme using Bayesian Information Criterion (BIC) (Fraley and Raftery 2003). A discriminant function analysis (DFA) was then performed on the *a priori* groupings of subspecific designations and then again using the groupings determined from the mclust results using the package MASS (Venables and Ripley 2002). Leave one out cross validation was used with the DFAs to determine the ability of the model to correctly classify both sets of groupings.

RESULTS

Molecular Analysis

A minimum of 6 subspecies, with a minimum of one and as many as 18 sample(s) per subspecies were included in each mitochondrial dataset. Despite significant effort, I was unable to obtain clean sequences for two of the 36 fresh tissue samples and nine of the 61 ancient tissue samples (Appendix 1). Across all seven datasets, none of the subspecies were found to be monophyletic (Figs. 5-11). In general, there was little support at the nodes (few posterior probabilities greater than 0.95) and low average genetic diversity within *D. heermanni* with average uncorrected *p* distances ranging from 1.07% to 2.45%) depending on the dataset (Appendix 5). Topological constraint analyses of fresh and ancient samples of *D. heermanni* rejected monophyly for all subspecies in the *Dloop* analysis (Appendix 6; a log difference above five is very strong evidence in favor of the better model - Kass and Raftery 1995). Monophyly of *D. h. berkeleyensis*, *D. h. goldmani*, *D. h. heermanni*, *D. h. jolonensis*, *D. h. swarthi*, *D. h. tularensis* was rejected in the *Cytb* analysis, monophyly of *D. h. arenae* and *D. h. dixoni* in the analysis of *Cytb* fresh and ancient tissues was not rejected as log likelihood scores were less than five (Appendix 6). Examining individual datasets, there was some support for monophyly for the subspecies *D. h. dixoni* (*ND2* and concatenated fresh tissue phylogenies; Figs. 6 and 8) and *D. h. tularensis* (*Dloop* and concatenated fresh tissue phylogenies; Figs. 7 and 8). However, in all other analysis these subspecies were not monophyletic (Figs. 5-7 and 9-11).

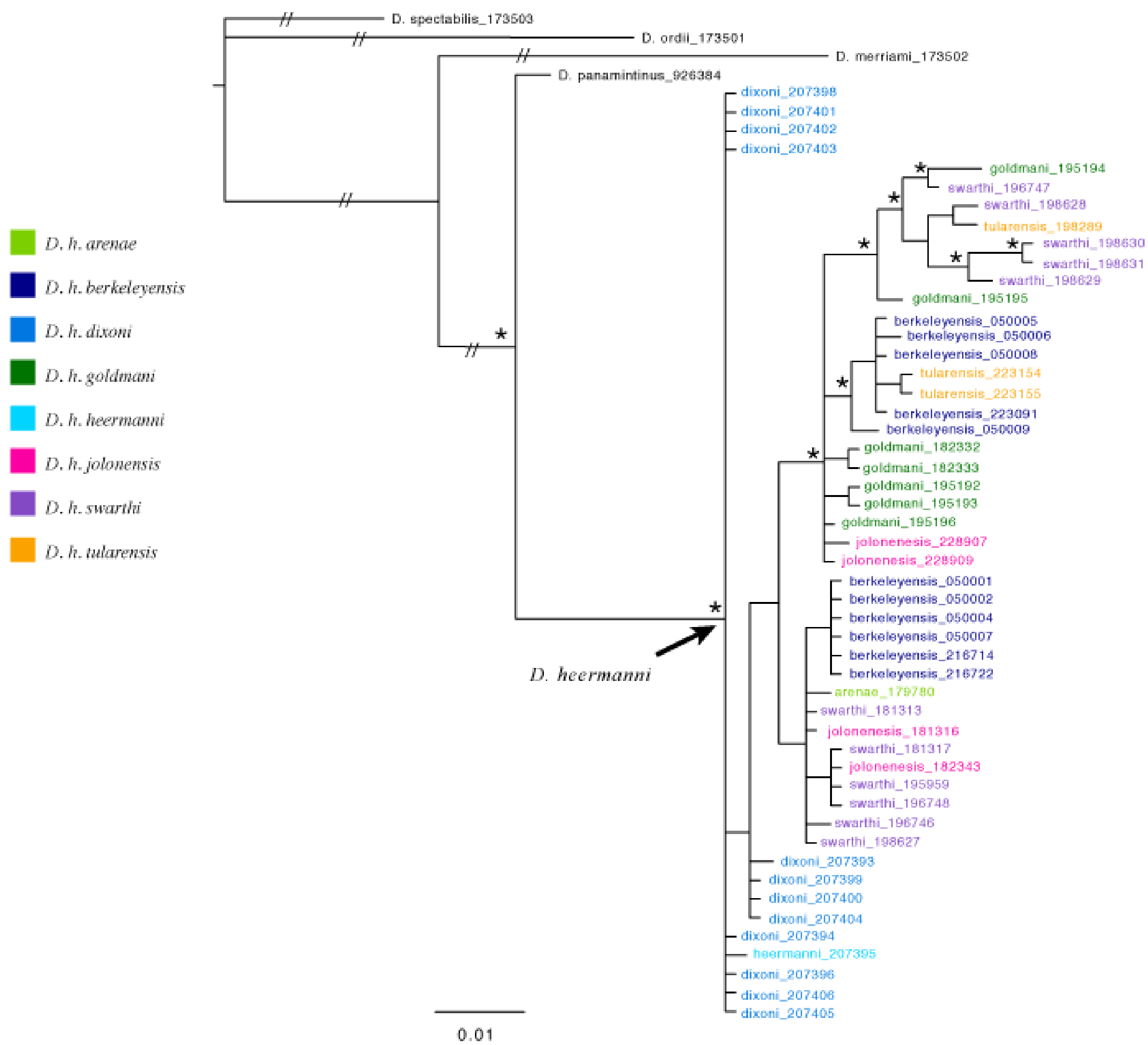

Figure 5. *Cytb* Bayesian phylogram for fresh tissue samples of *Dipodomys heermanni.* Posterior probabilities of 0.95 or greater are indicated with a *.

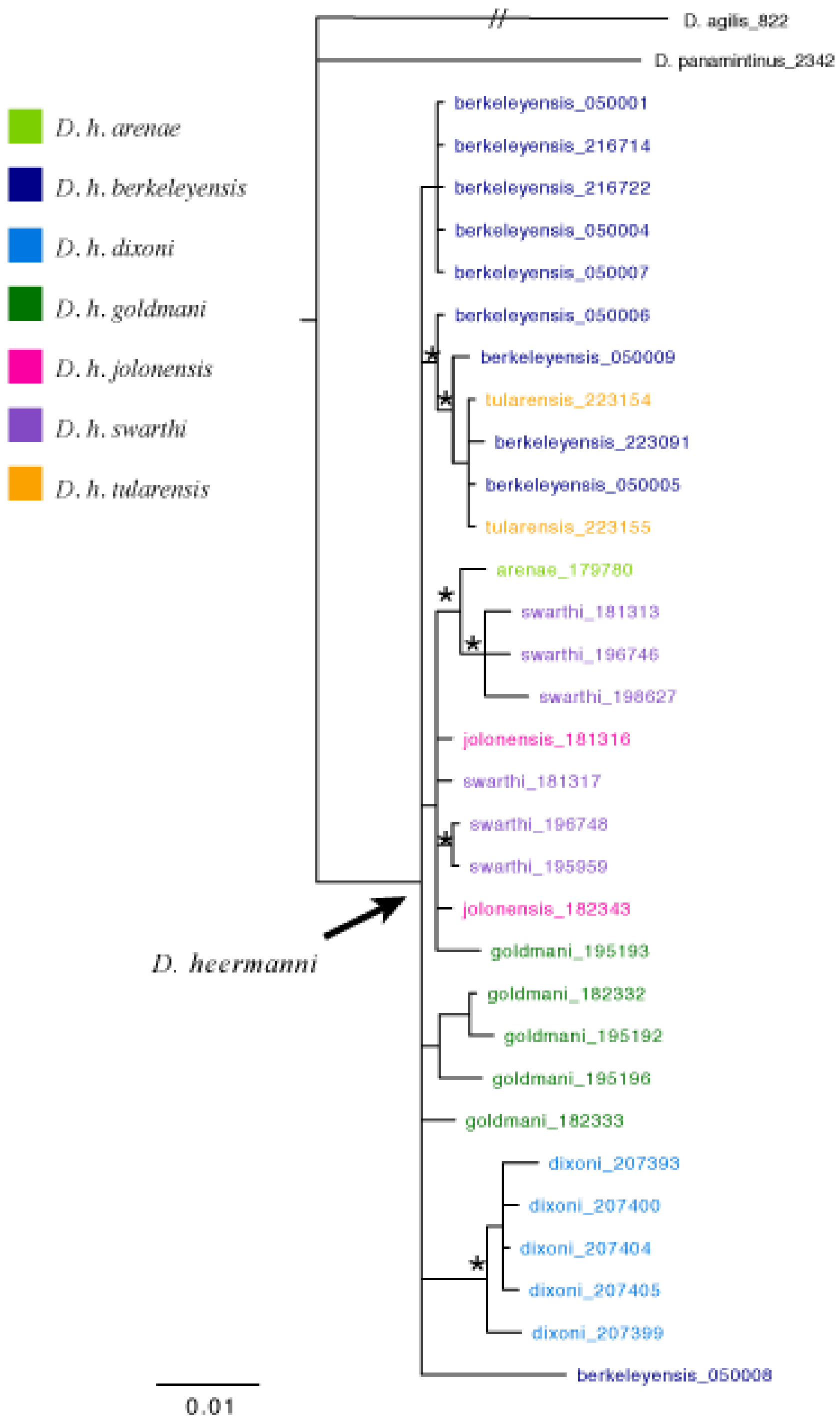

Figure 6. *ND2* Bayesian phylogram for fresh tissue samples of *Dipodomys heermanni.* Posterior probabilities of 0.95 or greater are indicated with a *.

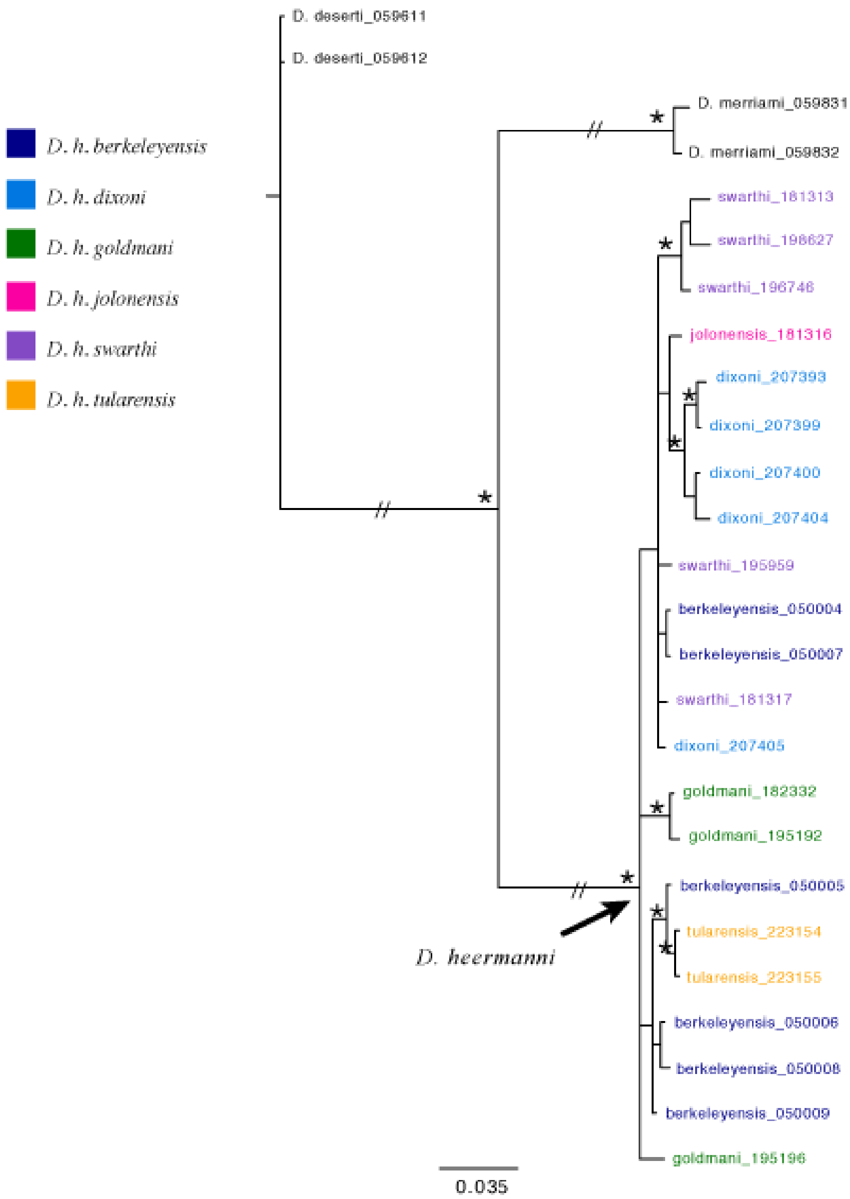

Figure 7. *Dloop* Bayesian phylogram for fresh tissue samples of *Dipodomys heermanni*. Posterior probabilities of 0.95 or greater are indicated with a *.

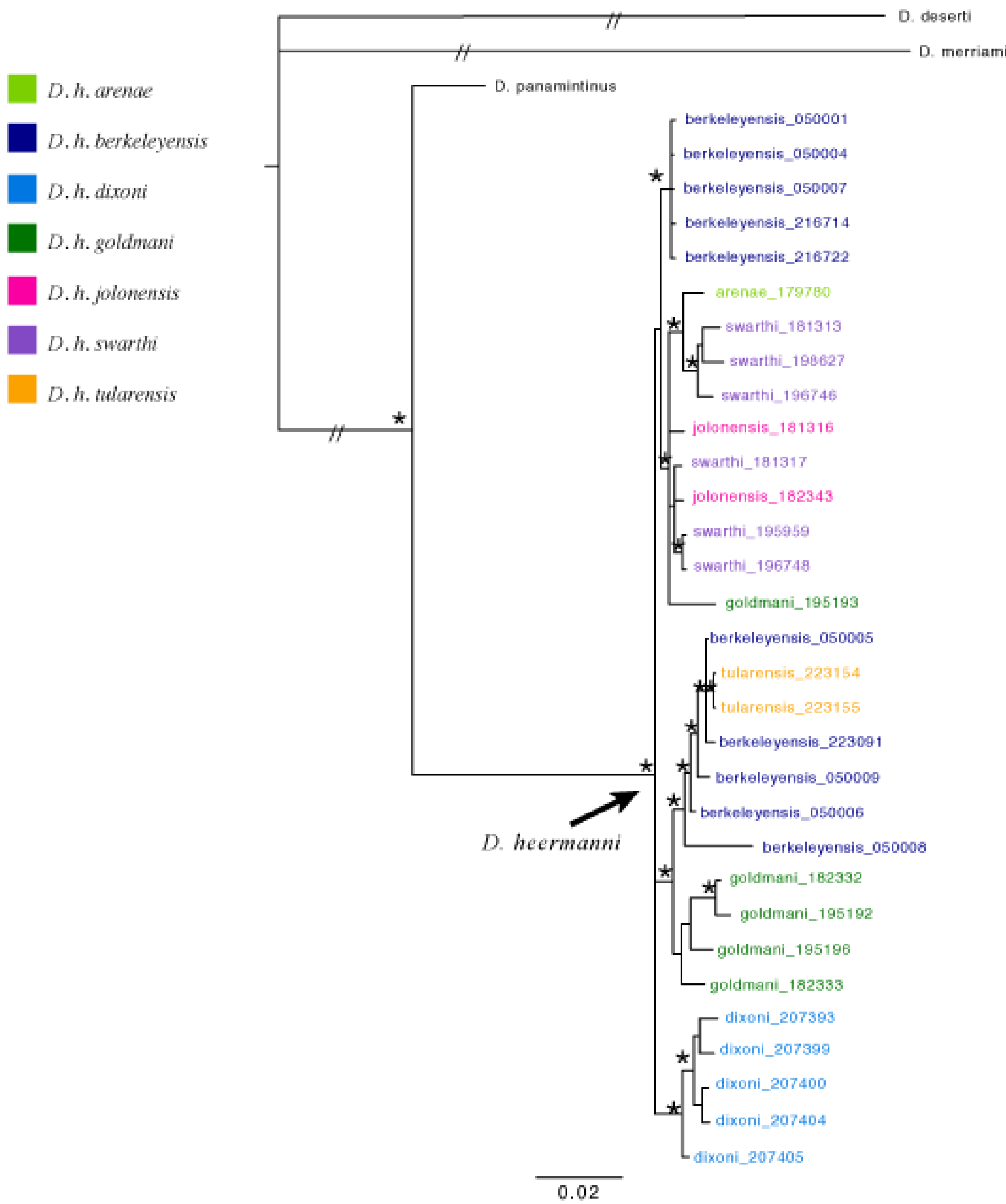

Figure 8. Concatenated Bayesian phylogram (including *Cytb*, *ND2*, and *Dloop*) for fresh tissue samples of *Dipodomys heermanni*. Posterior probabilities of 0.95 or greater are indicated with a *.

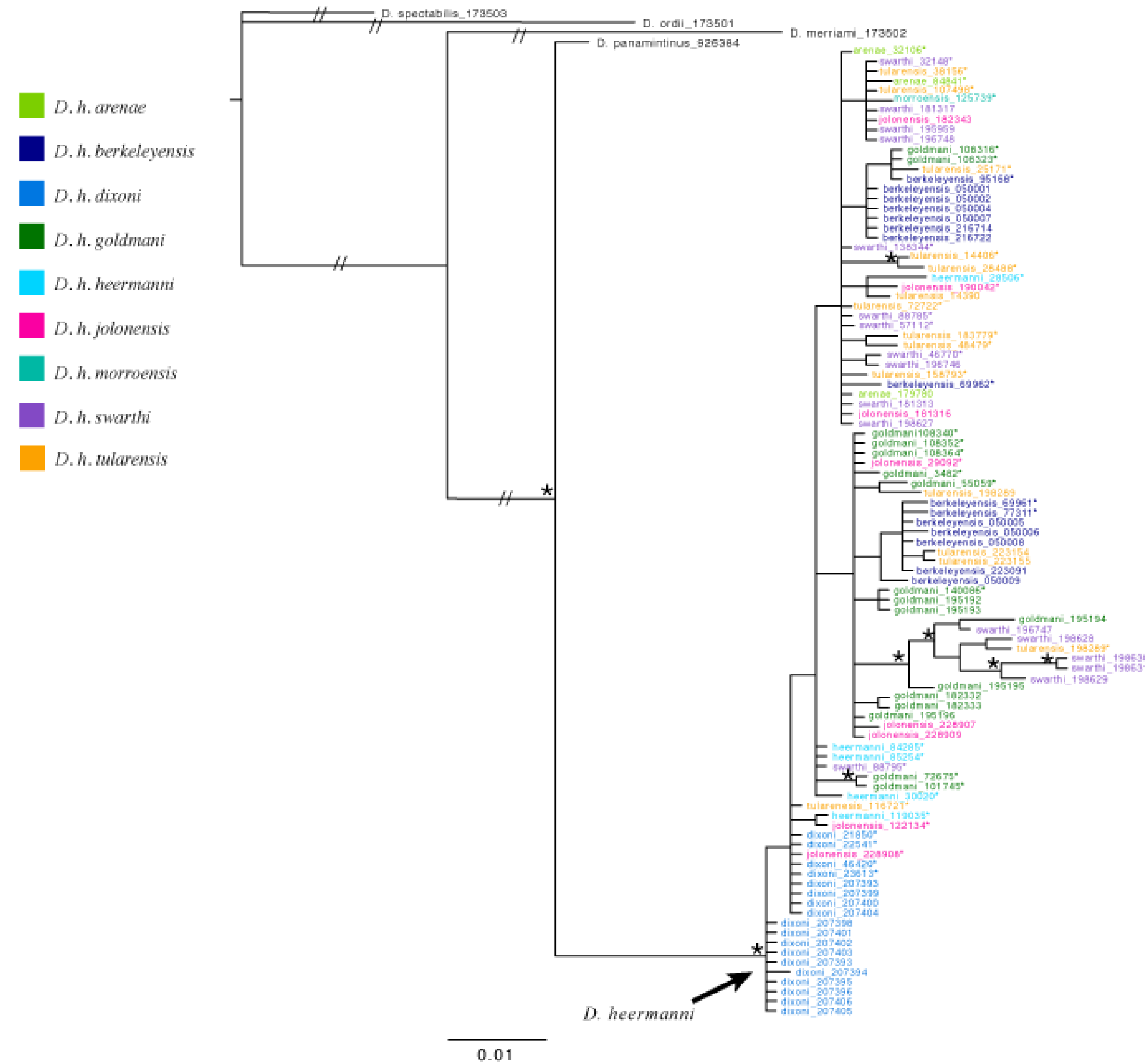

Figure 9. *Cytb* Bayesian phylogram for fresh tissue and ancient samples of *Dipodomys heermanni*. Posterior probabilities of 0.95 or greater are indicated with * and ancient samples are indicated by a colored * after the taxon name.

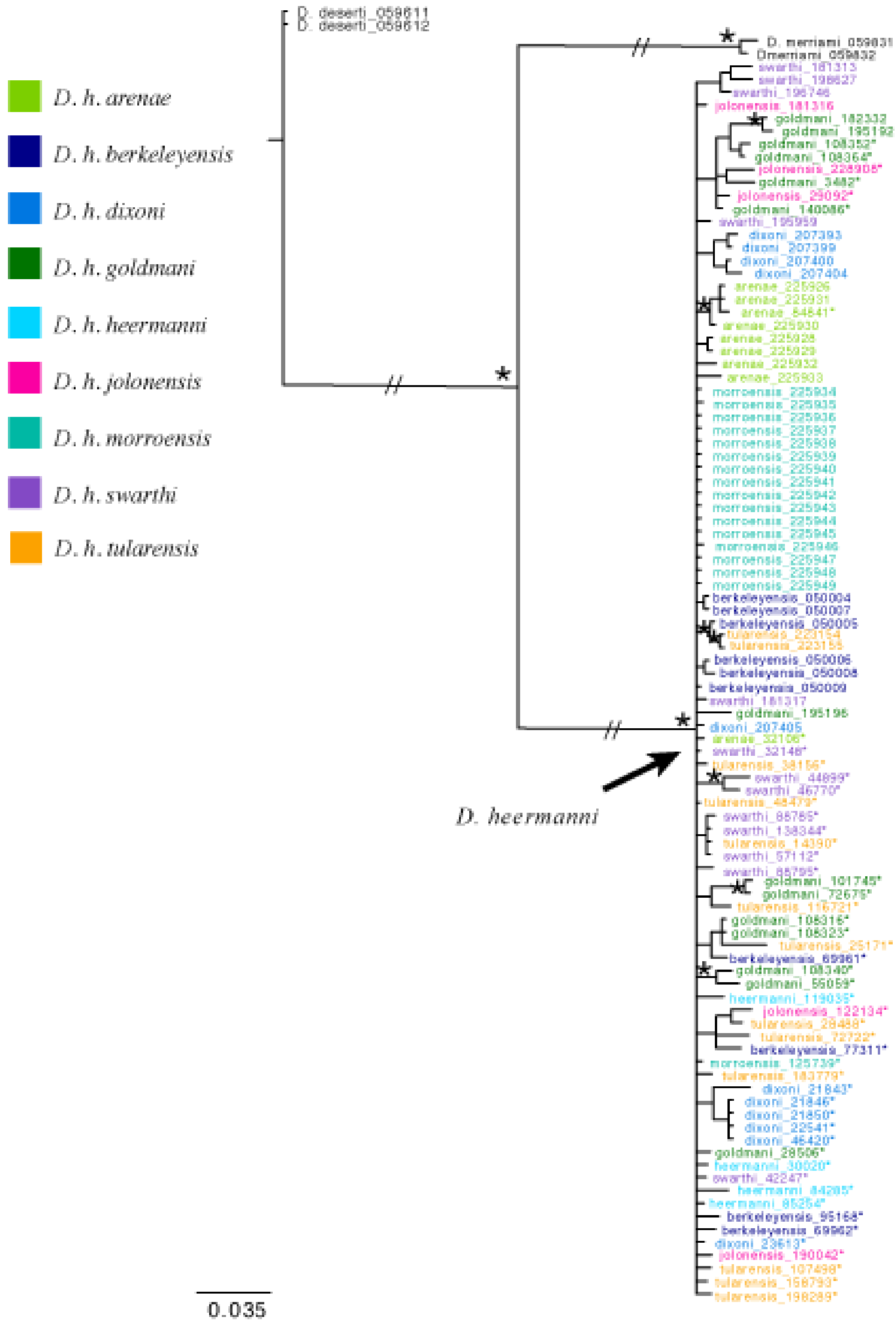

Figure 10. *Dloop* Bayesian phylogram for fresh tissue and ancient samples of *Dipodomys heermanni*. Posterior probabilities of 0.95 or greater are indicated with * and ancient samples are indicated by a colored * after the taxon name.

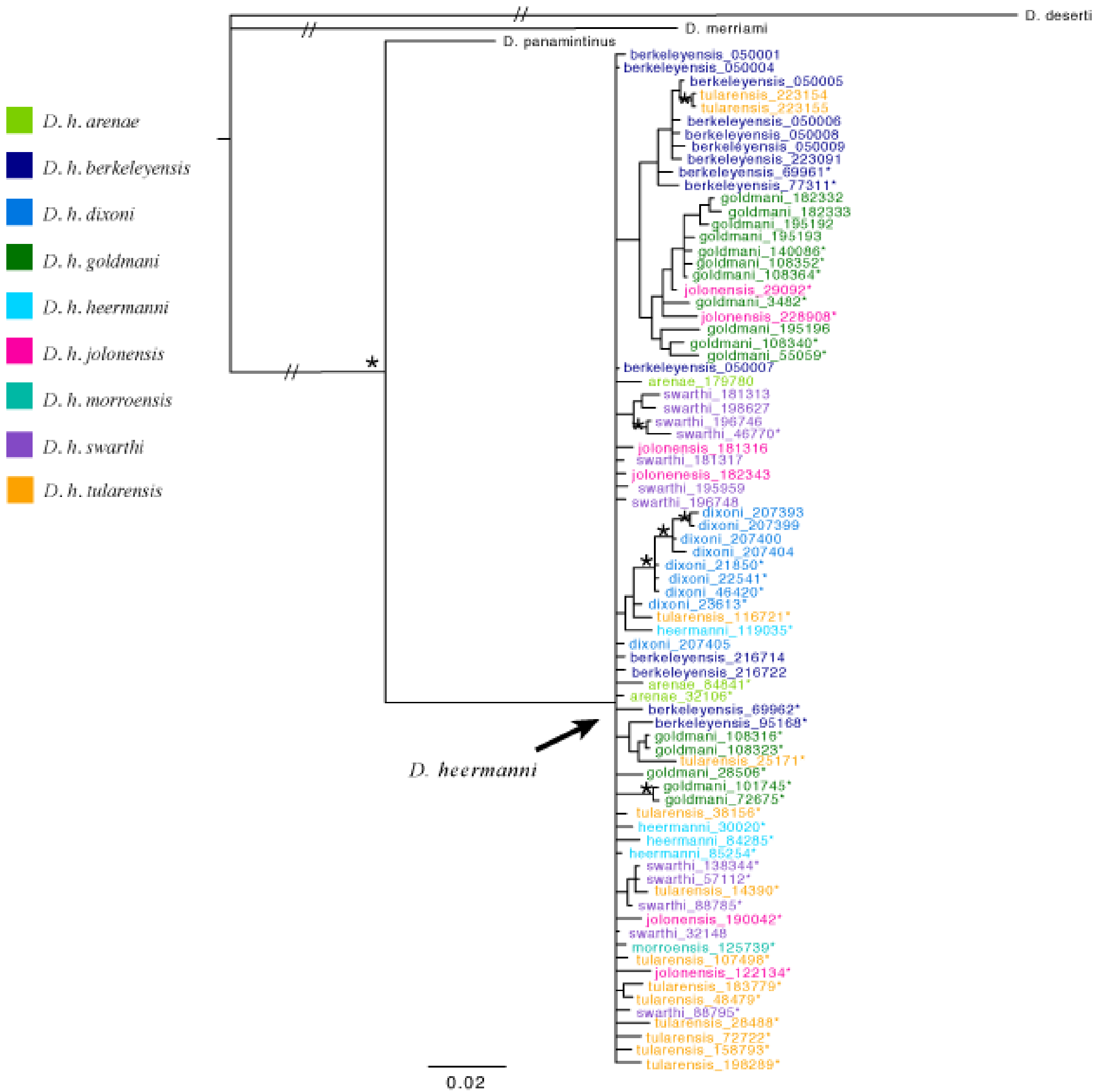

Figure 11. Concatenated Bayesian phylogram (including *Cytb* and *Dloop*) for fresh tissue and ancient samples of *Dipodomys heermanni*. Posterior probabilities of 0.95 or greater are indicated with * and ancient samples are indicated by a colored * after the taxon name.

For haplotype network analyses, each subspecies was represented by multiple haplotypes, which often did not group together (Figs. 12-16). Each subspecies shared a haplotype with another subspecies in at least one of the datasets (Figs. 12-16). The haplotype network for the *Cytb* gene for the fresh tissue samples dataset (50 specimens) produced 25 haplotypes and only *D. h. heermanni* and *D. h. dixoni* clustered somewhat separately (Fig. 12). There were five shared haplotypes for this dataset with *D. h. jolonensis* sharing haplotypes with *D. h. goldmani* and *D. h. swarthi*, *D. h. heermanni* sharing a haplotype with *D. h. dixoni*, and *D. h. berkeleyensis* sharing a haplotype with *D. h. tularensis* (Fig. 12). The haplotype network for the *ND2* gene for the fresh tissue samples dataset (31 specimens) produced 24 haplotypes and showed *D. h. dixoni* clustering separately (represented by five haplotypes; Fig. 13). The dataset showed one shared haplotype between *D. h. berkeleyensis* and *D. h. tularensis* (Fig. 13). The haplotype network for *Dloop* for the fresh tissue samples dataset (22 specimens) produced 20 haplotypes and showed *D. h. swarthi* and *D. h. goldmani* clustering somewhat separately (Fig. 14). Although there were no shared haplotypes for this dataset, subspecies were generally distributed throughout the network (Fig. 14).

The haplotype network for the *Cytb* gene for the fresh tissue and ancient samples dataset (96 specimens) produced 37 haplotypes and none of the subspecies clustered separately (Fig. 15). There were seven shared haplotypes for this dataset; the only subspecies that did not share haplotypes with other subspecies was *D. h. morroensis* (Fig. 15). The haplotype network for *Dloop* for the fresh tissue and ancient samples dataset (96 specimens) had 66 haplotypes and none of the subspecies clustered separately (Fig. 16). There were three shared haplotypes, two between *D. h. swarthi* and *D. h. tularensis* and one between *D. h. berkeleyensis* and *D. h. morroensis* (Fig. 16).

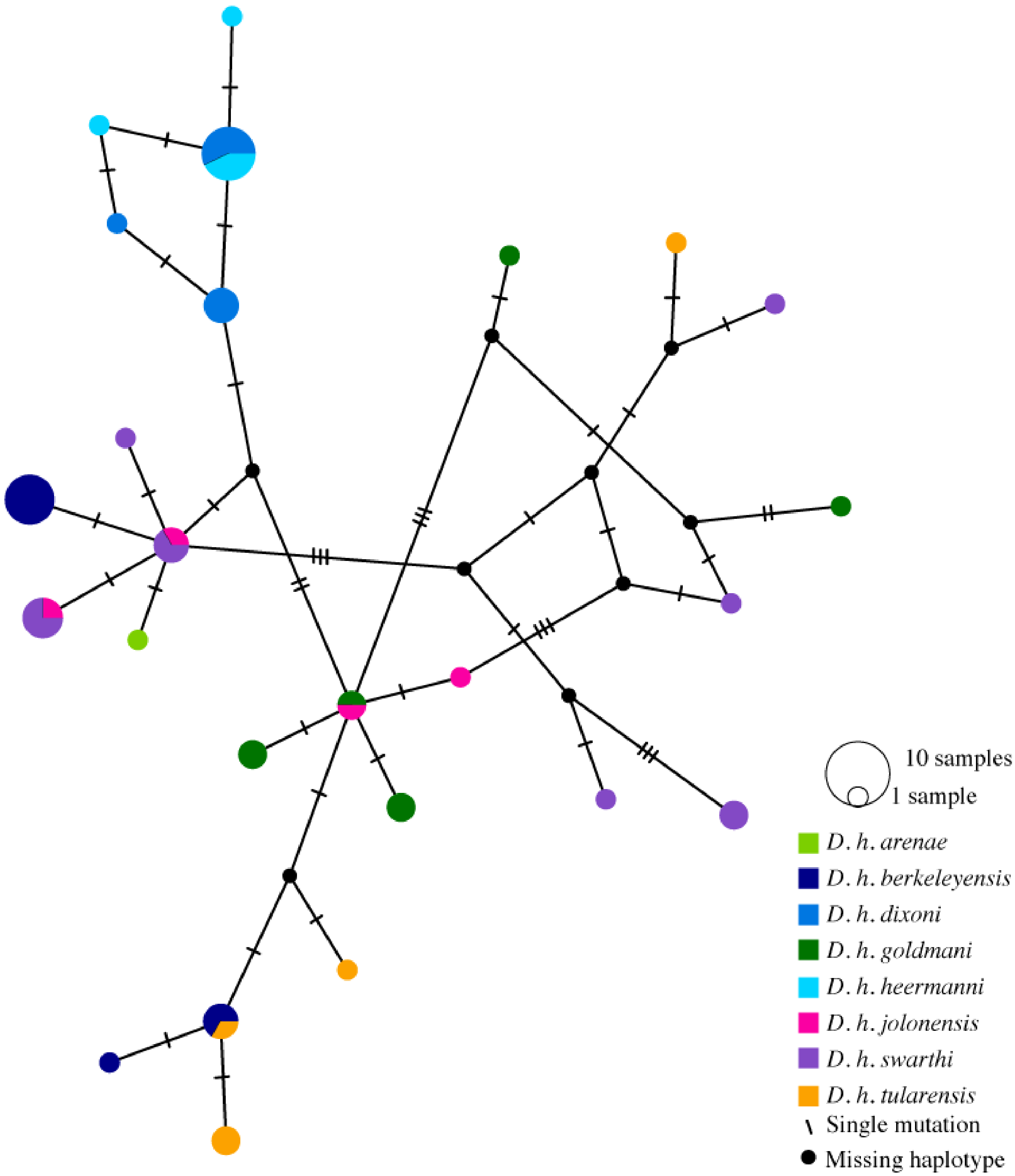

Figure 12. Haplotype network for the *Cytb* gene for fresh tissue samples of *Dipodomys heermanni*.

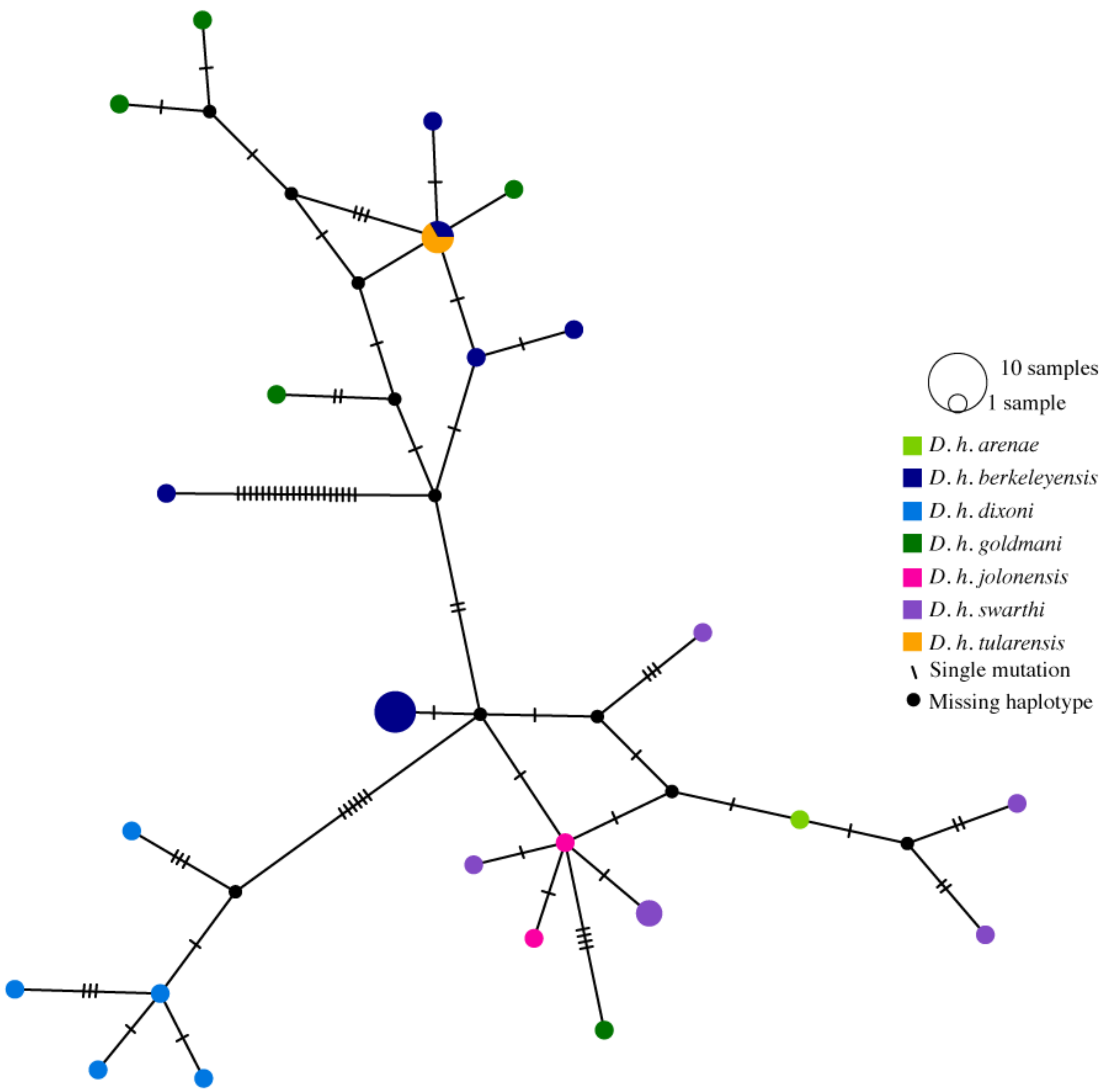

Figure 13. Haplotype network for the *ND2* gene for fresh tissue samples of *Dipodomys heermanni*.

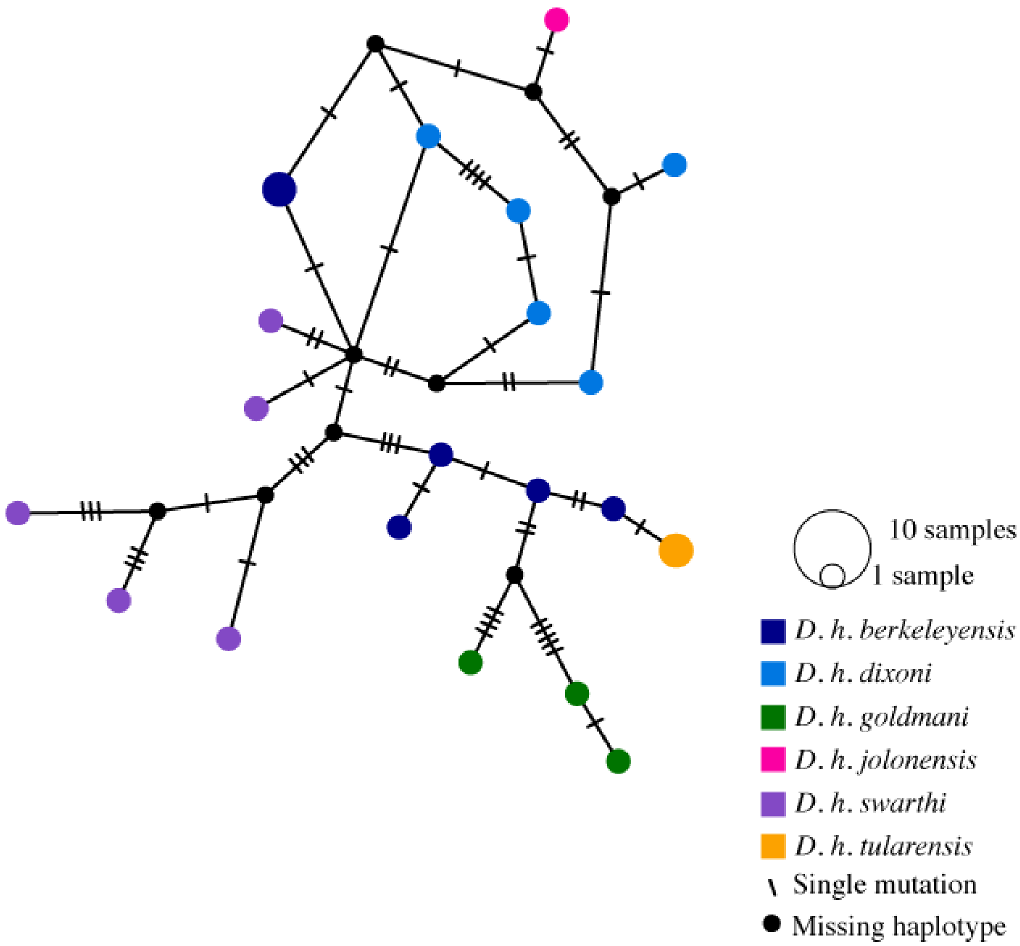

Figure 14. Haplotype network for *Dloop* for fresh tissue samples of *Dipodomys heermanni*.

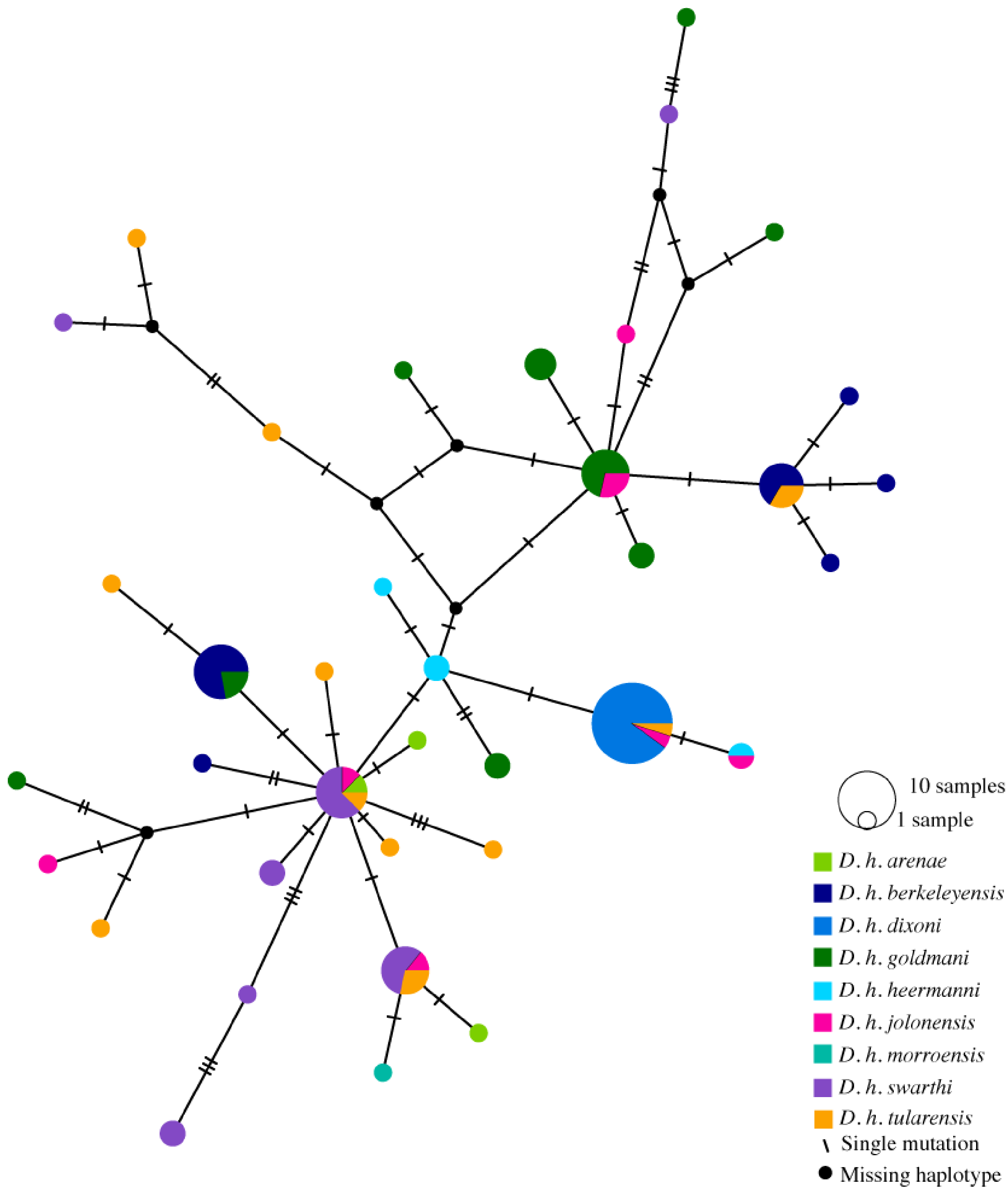

Figure 15. Haplotype network for the *Cytb* gene for fresh tissue and ancient samples of *Dipodomys heermanni*.

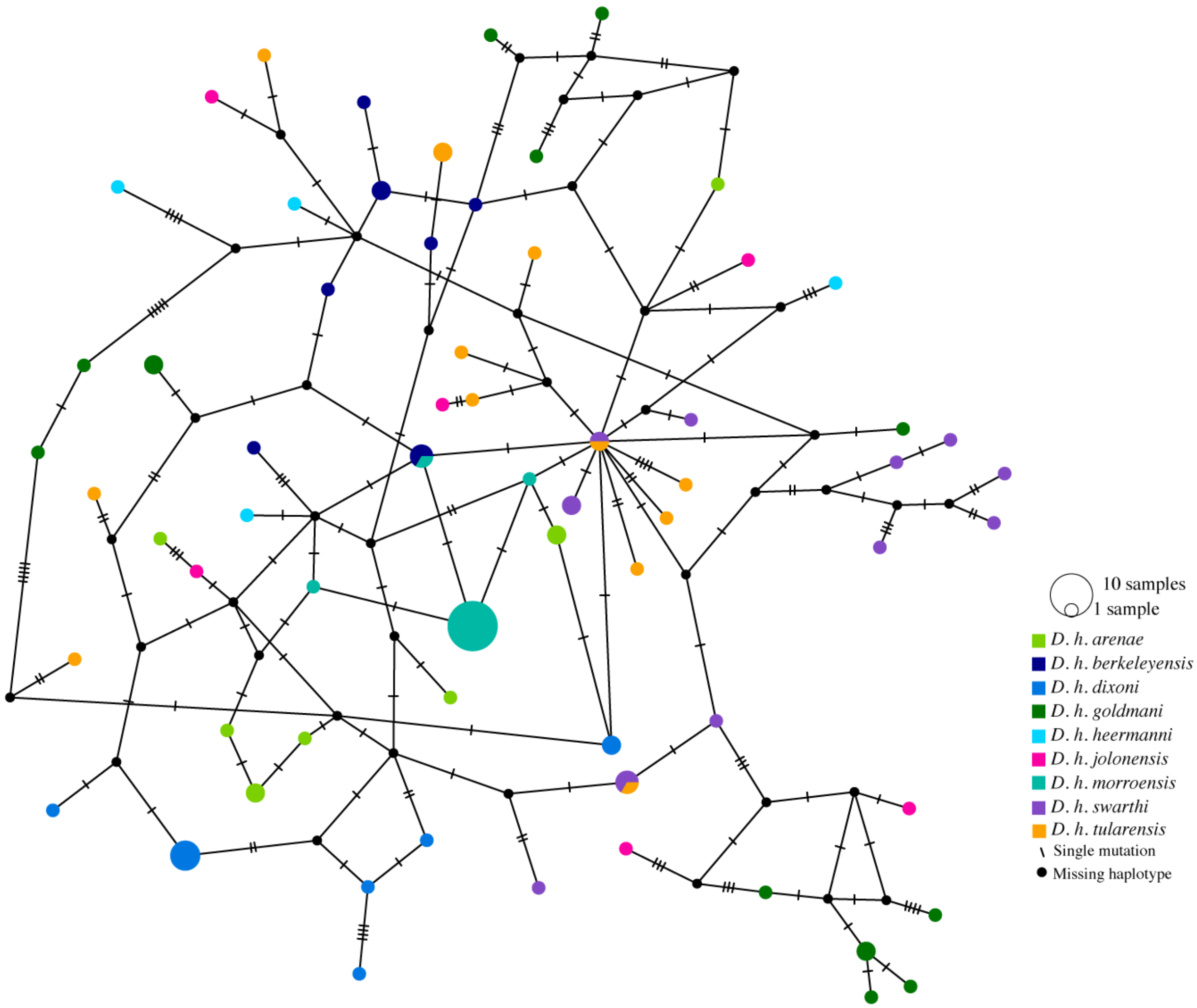

Figure 16. Haplotype network for *Dloop* for fresh tissue and ancient samples of *Dipodomys heermanni*.

Morphological Analysis

Based on the quality of the skulls and unique geographic locations, 203 specimens were used in the analysis of the dorsal view and 196 specimens were used in the analysis of the ventral view (Appendix 2). No evidence of sexual dimorphism was found in the dorsal (t = -0.38718, *P* = 0.6986) or ventral (t = 0.53921, *P* = 0.5898) views. All subsequent analyses therefore used a combined dataset of male and female specimens.

Fifteen principal components showed 95% of the variation in the dorsal view, whereas nineteen principal components showed the same percentage of the variation in the ventral view (Appendix 7). Visualization of the first few principal components shows significant overlap of all nine subspecies for both the dorsal and ventral views (Figs. 17 and 18). The best mclust model determined by BIC resulted in four distinct clusters (cluster categories 1-4) for both views with the VVI model, which is distributed diagonally with variable volume and shape. This model primarily partitioned the individuals into two groups for both the dorsal (84.73% of all specimens) and ventral (72.96% of all specimens) views, with the remainder clustering into two smaller groups (Table 2). The majority of the specimens in the dorsal view fell into cluster category 1, while the ventral view had a little more variation (Table 3). None of the cluster categories grouped geographically, nor did the dorsal cluster categories match the ventral categories (Figs. 19-21). The DFAs showed little support for current subspecies designations, with an overall prediction accuracy of 20.69% for the dorsal view and 26.02% for the ventral view (Appendix 8). The DFA predicted an overall accuracy of 88.67% for the four clusters created by mclust for the dorsal view and 84.18% for the four clusters created by mclust for the ventral view (Appendix 8).

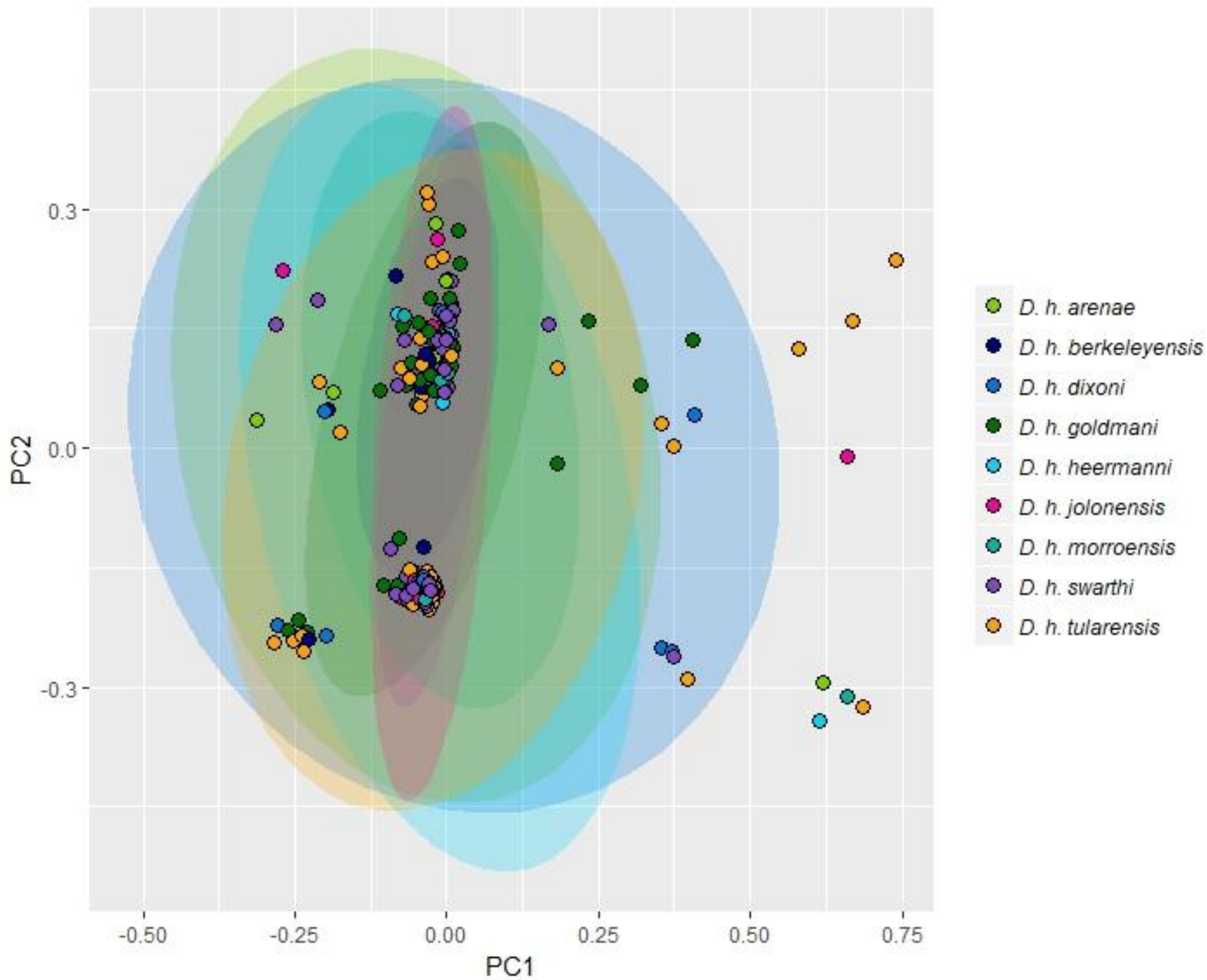

Figure 17. PCA for the dorsal view of *Dipodomys heermanni* skulls used in the morphological analysis.

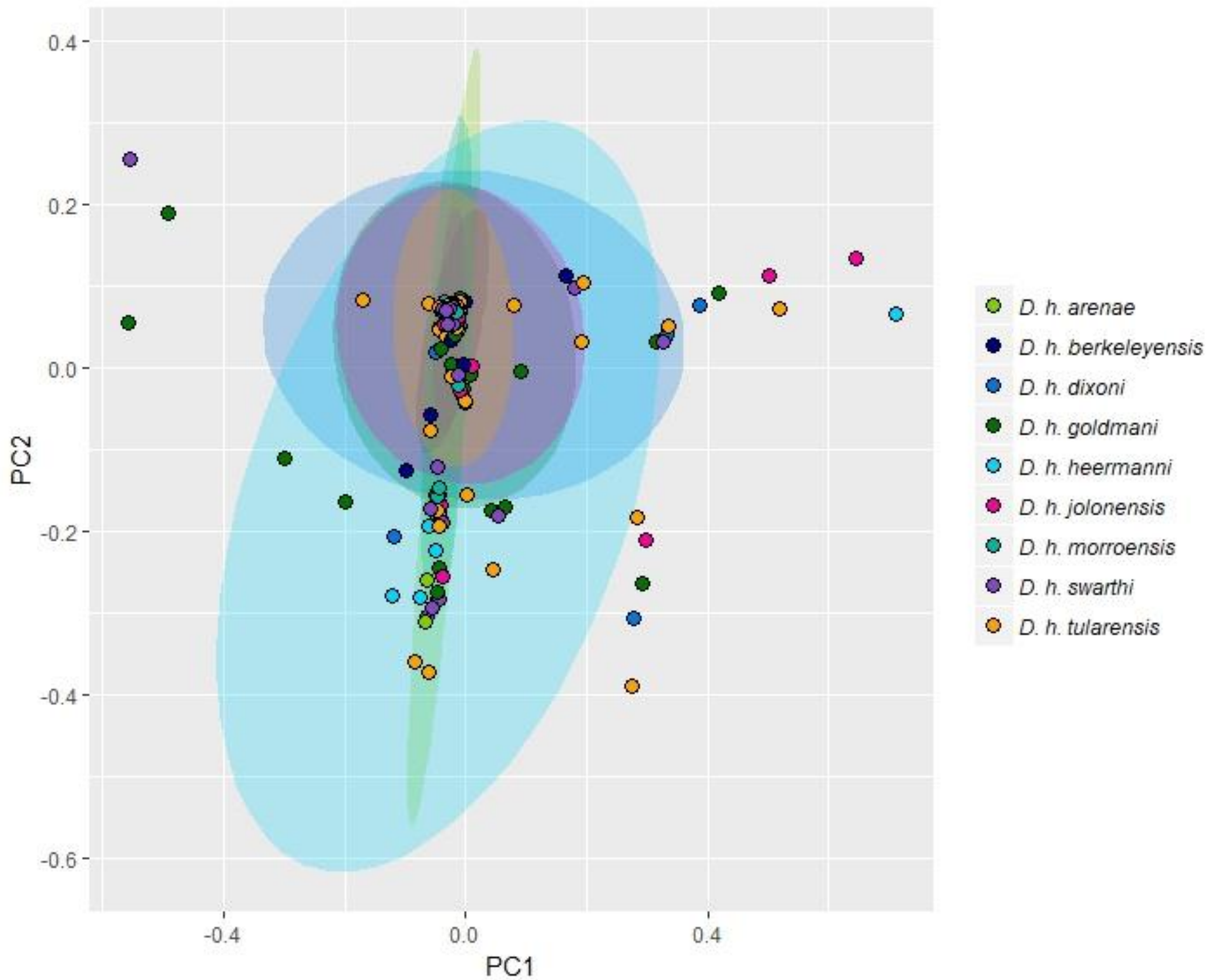

Figure 18. PCA for the ventral view *Dipodomys heermanni* skulls used in the morphological analysis.

Table 2. Cluster categories using mclust for the dorsal and ventral views of *Dipodomys heermanni* skulls used in the morphological analysis.

Cluster Categories	Individuals	Percentage
Dorsal View		
1	128	63.05
2	16	7.88
3	15	7.39
4	44	21.67
Total	203	100
Ventral View		
1	77	39.29
2	66	33.67
3	36	18.37
4	17	8.67
Total	196	100

Table 3. Individuals in each cluster category as determined by mclust, separated by subspecies, for the dorsal and ventral views of *Dipodomys heermanni* skulls used in the morphological analysis.

Cluster Categories	**1**	**2**	**3**	**4**
Dorsal View				
D. h. arenae	8	0	1	1
D. h. berkeleyensis	10	0	3	1
D. h. dixoni	9	0	3	0
D. h. goldmani	24	4	0	12
D. h. heermanni	3	2	1	1
D. h. jolonensis	10	2	1	4
D. h. morroensis	4	1	0	3
D. h. swarthi	32	0	2	13
D. h. tularensis	28	7	5	9
Ventral View				
D. h. arenae	3	3	2	1
D. h. berkeleyensis	8	3	1	2
D. h. dixoni	4	5	2	0
D. h. goldmani	11	14	6	6
D. h. heermanni	5	2	0	0
D. h. jolonensis	4	4	6	3
D. h. morroensis	4	2	1	0
D. h. swarthi	16	16	10	2
D. h. tularensis	22	17	8	3

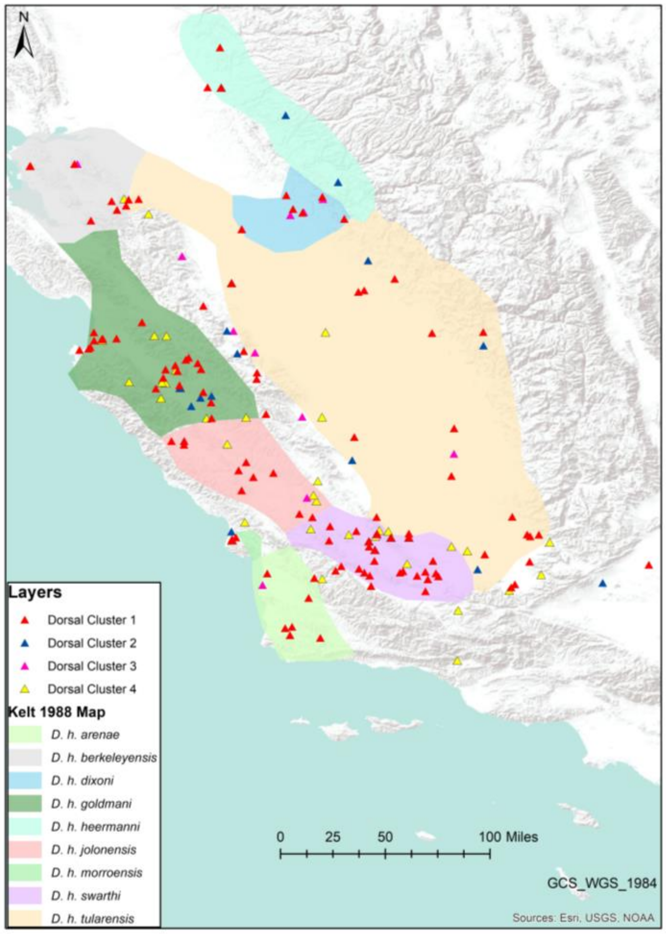

Figure 19. Cluster categories for the dorsal view of *Dipodomys heermanni* skulls used in the morphological analysis indicated by filled triangles, overlain with Kelt (1988) subspecific distribution map (shaded regions)**.**

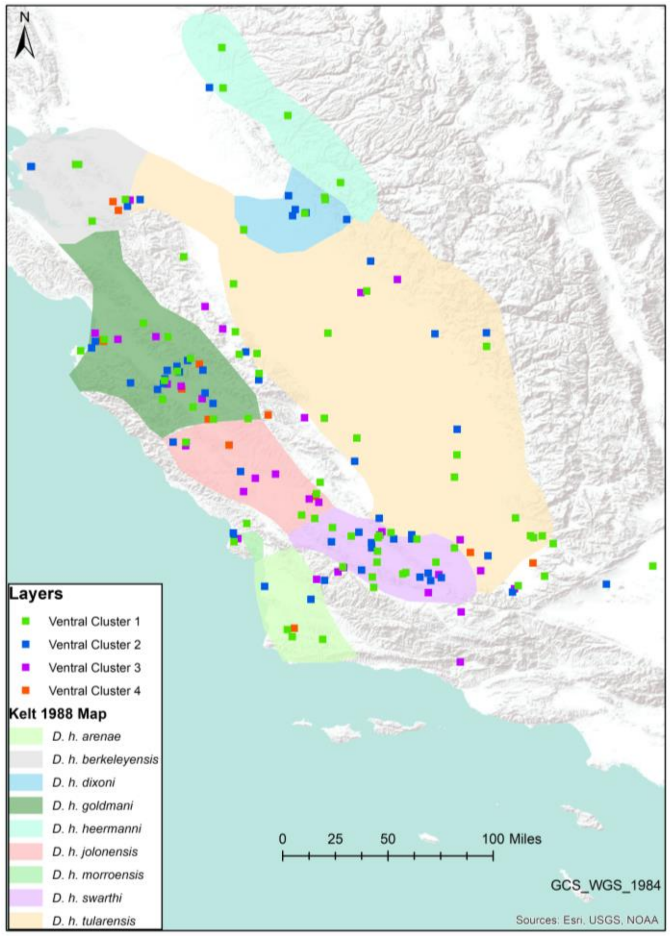

Figure 20. Cluster categories for the ventral view of *Dipodomys heermanni* skulls used in the morphological analysis indicated by filled squares, overlain with Kelt (1988) subspecific distribution map (shaded regions)**.**

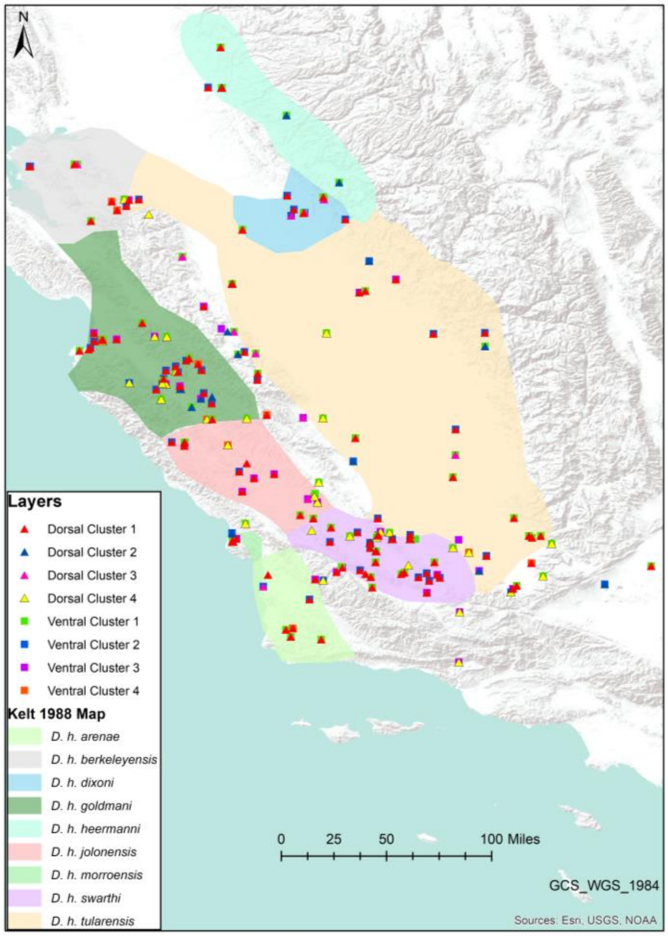

Figure 21. Cluster categories for the dorsal and ventral views of *Dipodomys heermanni* skulls used in the morphological analysis indicated by filled triangles and squares (respectively), overlain with Kelt (1988) subspecific distribution map (shaded regions)**.**

DISCUSSION AND CONCLUSIONS

Subspecies are often regarded as populations that have made steps towards becoming species and have a degree of isolation, usually geographic, from other such populations (Wilson and Brown 1953; Lidicker 1962; Braby et al. 2012; Patton and Conroy 2017). Examination of subspecific taxonomy should include an analysis of genetic and morphological differentiation, as well as assessment of geographic isolation (Lidicker 1962; Braby et al. 2012). Following these recommendations, I conducted a search for genetic and morphological variation across all nine subspecies within *D. heermanni*. Neither morphological or molecular data supported the current subspecific taxonomy of *D. heermanni*. The use of molecular analysis and geometric morphometrics did not inflate the number of subspecies (contra Garnett and Christidis 2017).

Although this study essentially uses one molecular marker (mitochondrial DNA), mitochondrial markers that have proven useful at the intraspecific level in studies of other rodent species, especially as a first attempt to examine genetic differentiation across the entire geographic distribution of the species (e.g., Smith and Patton 1991; Bradley and Baker 2001; Matocq and Villablanca 2001; Alexander and Riddle 2005; Andersen and Light 2012; Light et al. 2016). My molecular results did not reveal any of the *D. heermanni* subspecies as being monophyletic, with haplotype sharing among subspecies and a lack of subnetworks or clusters corresponding to subspecies or unique genetic groups (Appendix 6, Figs. 5-16). Although there was support for monophyly for the subspecies *D. h. dixoni* (Figs. 6 and 8) and *D. h. tularensis* (Figs. 7 and 8) when examining individual datasets, this was possibly due to a low sample size (five and two samples, respectively); in all other analyses, the monophyly of *D. h. dixoni* (Figs. 5, 7, and 9-11) and *D. h. tularensis* (Figs. 5-6 and 9-11) was not supported. Alternatively, it is possible that missing data may have resulted in lack of subspecific monophyly. Specimens were included in the concatenated analyses if two of the three mitochondrial markers (for the fresh tissue samples) and two of the two markers (for the ancient samples) successfully sequenced, resulting in one missing sequence for *Cytb* and nine missing sequences for *Dloop* in both concatenated analysis. Some studies argue that missing data can be included in phylogenetic analyses so long as the number of characters analyzed is not too low (Wiens and Moen 2008; Wiens and Morrill 2011; Roure et al. 2012). Alternatively, others argue that missing data can introduce parameter misestimations, decrease resolving power, and reduce the detection of multiple substitutions resulting in incorrect phylogenetic results (Roure et al. 2012). Additional error could come in the form of nuclear mitochondrial (*numt*) gene sequences, and their accidental amplification in addition to or instead of the targeted mitochondrial sequence (Zhang and Hewitt 1996; Sorenson and Quinn 1998; Richly and Leister 2004; Thalmann et al. 2004; Kim et al. 2006; Pontius et al. 2007; Davis et al. 2010). *Numts* have been reported in more than 60 animals and plant species and are most commonly described as fragments of less than 600 bp (Zhang and Hewitt 1996; Herrnstadt et al. 1999; Bensasson et al. 2001; Kim et al. 2006). Ancient samples are prone to *numts* (Willerslev and Cooper 2005). Furthermore, ancient samples are particularly sensitive to mutations as gene amplification in ancient samples often is performed for small fragments often resulting in PCR-induced mutations (Pusch and Bachmann 2004; Willerslev and Cooper 2005). Even with careful protocols and procedures, *numts* and mutations can occur and go undetected resulting in incorrect topologies (Gilbert et al. 2005; Willerslev and Cooper 2005).

Notably, *Cytb*, *ND2*, and *Dloop* are not informative in differentiating among *D. heermanni* subspecies or revealing any substantially differentiated mitochondrial clades. Matocq and Villablanca (2001) also discovered low genetic diversity in their mitochondrial data of *D. h. morroensis* and attributed this to historical processes rather than a recent bottleneck. Perhaps this is not surprising given the close affinity between *D. heermanni* and *D. panamintinus* (Grinnell 1922; Lidicker 1960; Johnson and Selander 1971; Stock 1974) and the recent divergence of less than one million years ago between these two taxa (Hafner et al. 2007). The relatively recent emergence of *D. heermanni* may explain the lack of mitochondrial variation across the geographic range of this species. In contrast, *Cytb* and *Dloop* have proven successful in showing divergence in other *Dipodomys* species at a population level. Using *Cytb*, Fernández et al. (2012) found 9.8% divergence between two clades of *Dipodomys phillipsii* resulting in the recognition of a new species. Good et al. (1997) found high intra- and interpopulation variation in *Dloop* among 95 specimens and nine localities of *Dipodomys ingens*. Additionally, Álvarez-Castañeda et al. (2009) were able to find considerable variation in *Dipodomys merriami* across the Baja Peninsula (similar to previous studies; Riddle et al. 2000). Thus, the mitochondrial markers used in this study have the potential to detect variation, if present, within *Dipodomys* species. Future work examining *D. heermanni* phylogeography should consider the use of more variable regions of *Dloop* as well as additional population markers such as microsatellites or SNPs. This is especially important because some studies using microsatellites have revealed a greater amount of variation than mitochondrial markers (Ritz et al. 2000; Eizirik et al. 2001; Hanfling et al. 2002; Hausdorf et al. 2011).

For examination of morphological variation, I was cognizant of the original characteristics used to classify *D. heermanni*, taking them into consideration in my assessment of the species, as recommended by Patton and Conroy (2017). For example, my morphological methods included an analysis of the breadth of the skull, size of the bullae, length of the nasals, size of the supraoccipital, and size of the maxillary, as these characteristics were described by Boulware (1943) and Grinnell (1922) as being important in distinguishing among subspecies (Table 1). Similarly, dental characteristics that could differentiate among *Dipodomys* species were also captured (Carrasco 2000). The morphological results were comparable to the molecular results in that they did not support clusters based on subspecific taxonomy. While there was support for *D. heermanni* clustering into four categories, the clusters were inconsistent between the ventral and dorsal views and the clustering was unrelated to geographic distribution as none of the clusters were geographically isolated (Figs. 19-21).

My morphological analysis, geometric morphometrics, should capture differences in cranial characteristics at a finer scale among taxa because geometric morphometrics is particularly useful in capturing small localized changes in shape as it is more sensitive than traditional morphometrics (Adams et al. 2004, 2013; Breno et al. 2011; Schmieder et al. 2016). Importantly, geometric morphometrics has proven useful in differentiating among numerous rodents at specific and subspecific levels, and across geographic scales (e.g., Reis et al. 2002; Cardini and O'Higgins 2004; Cordeiro-Estrela et al. 2006; Breno et al. 2011; Yazdi and Adriaens 2011; Quintela et al. 2016; Kubiak et al. 2017). It is possible that my landmark and semilandmark schemes of the dorsal and ventral views of the skulls may have missed variation in other parts of the skull. Thus, future work could include a geometric morphometrics analysis of additional views of *D. heermanni* skulls, including a lateral view and views of the lower jaw. Future studies also could include analysis of pelage color and markings, as these characters were not included in this study (e.g., Brown et al. 2007; Musiani et al. 2007; Álvarez-Castañeda et al. 2009).

This study was able to gain some insight and build upon past work done on the federally and state listed *D. h. morroensis*. Due to population declines resulting from habitat loss, *D. h. morroensis* was listed as endangered pursuant to the U.S. Endangered Species Conservation Act in 1970 (USFWS 1970), the California Endangered Species Act in 1971(CESA 1971), and the U.S. Endangered Species Act in 1973 (ESA 1973), and has not been caught in the wild since 1985 despite considerable effort and investment (Villablanca 2009; Kofron and Villablanca 2016). In the Draft Revised Recovery Plan for the Morro Bay Kangaroo Rat (1999), one of the recovery strategies is to focus research efforts to better understand the basic biology, life history, and especially the genetics of this subspecies. While prior genetic studies supported that *D. h. morroensis* is genetically distinct, these studies only compared *D. h. morroensis* to a maximum of four other *D. heermanni* subspecies (Matocq and Villablanca 2001; Kofron and Villablanca 2016). My study did not find *D. h. morroensis* to be genetically or morphologically distinct. There was no support for monophyly of *D. h. morroensis* in any of the molecular analyses (Figs. 5-16) and one *D. h. morroensis* specimen even shared a haplotype with *D. h. berkeleyensis* (Fig. 16). Notably, 16 of the 17 *D. h. morroensis Dloop* sequences included in this study were downloaded from GenBank. Unlike the samples that we sequenced ourselves, the GenBank samples were not culled based on their geographic locality; they were downloaded based on availability to increase our sample size for the less represented subspecies. These *D. h. morroensis* specimens all have the same geographic locality and not surprisingly were represented by a small number of haplotypes (Fig. 16).

The present study also was able to gain additional information about *D. h. berkeleyensis*, which is not state or federally listed but is described as “presumed extinct” in The U.S. Fish and Wildlife Service (USFWS) Draft Recovery Plan (2002) for chaparral and scrub community species east of San Francisco Bay (USFWS 2017). The recovery plan states that the immediate goal for *D. h. berkeleyensis* is to confirm its status and if extant populations of species are discovered, the ultimate goal would be to ensure the long-term conservation of those populations. The recovery plan also says that if species are rediscovered then conservation actions should include actions such as protection, reducing threats, and genetic analysis (USFWS 2002). Alameda County, in particular, has interest in determining the status of *D. h. berkeleyensis*; the Alameda Watershed Habitat Conservation Plan lists *D. h. berkeleyensis* as a "no take" species (SFPUC 2010-2012). However, given the lack of research and data on *D. h. berkeleyensis*, no precautions are being enforced for its protection. In 2004, a kangaroo rat collected by Mr. Joseph DiDonato (owner of Wildlife Consulting and Photography) was confirmed by Dr. William Lidicker as possibly being the supposedly extinct *D. h. berkeleyensis* based on its collection locality (Fig. 1). Following this, additional individuals were captured by Mr. DiDonato, a skin or hair sample was taken, and the specimens were released. Many of these specimens are included in this study (labeled with a BE number; Appendix 1). Unpublished work by Drs. Doug Bell (Wildlife Program Manager at East Bay Regional Park District) and Per Palsböll (University of Groningen) examining mitochondrial data showed that there was little genetic variability within *D. h. berkeleyensis*, but some differentiation between *D. h. berkeleyensis* and *D. h. tularensis*. However, my results show that *D. h. berkeleyensis* is not genetically or morphologically unique compared to the other eight *D. heermanni* subspecies.

California has the highest endemism of mammal species out of any state in the country, with six of the 17 endemic mammals belonging to the genus *Dipodomys* (CDFG 2003), including *D. heermanni*. The San Joaquin Valley region is one of the areas with the highest mammalian endemism in California, likely owing to an active biogeography history, particularly the build-up of mountain ranges that surround the valley (CDFG 2003). Approximately seven million years ago, the uplifting of the Transverse Range, Sierra Nevada Mountain Range, and Coast Range resulted in a period of molecular differentiation and major genetic splits in most animal taxa in California (Calsbeek et al. 2003). Between 4,000 and 8,000 years ago, there may have been a brief moment in history where dry conditions allowed migration of species from the east side of the Sierra Nevada Mountain Range to the San Joaquin Valley (CDFG 2003). Since then, the arid grasslands and scrub habitat of the San Joaquin Valley have become geographically isolated for many species, potentially including *D. heermanni* (CDFG 2003). Further isolating *D. heermanni* are the many mountain ranges surrounding the species (Fig. 1). Today, the high elevation of the Sierra Nevada Mountain Range (with peaks above 10,000 feet) create a cool moist environment, which is unlike the shallow and well-draining soil with little vegetation, sandy valley floors, or coastal plains that *D. heermanni* prefers (Fitch 1948; Kelt 1988; CDFG 2003). To the west, the Santa Cruz Mountains and coastal edge of the Santa Lucia Range are characterized by coast redwoods, possibly creating an unfavorable habitat for *D. heermanni* (CDFG 2003). To the north, a network of waterways in the San Francisco Bay and eastward likely create a barrier for *D. heermanni*, a species averse to water (Grinnell 1922). Additionally, the San Francisco Bay is a particularly dense urban area leaving little habitat for *D. heermanni* (CDFG 2003). To the south, in addition to the Sierra Nevada Mountain Range, the range of *D. heermanni* may be disrupted by the Santa Inez River, which intersects the Transverse Ranges (Boulware 1943). Lastly, the Coast Ranges were uplifted approximately two million years ago (Kuchta et al. 2009). Early distribution maps show *D. heermanni* presented as a ring around a portion of the Coast Ranges of California (Fig. 1, Hall 1981; Kelt 1988), implying that the Coast Ranges may form a barrier to species dispersal. However, mapping of museum localities places *D. heermanni* inside of the ring (Fig. 1); thus *D. heermanni* is not restricted to the original subspecies boundaries defined by Hall (1981) and Kelt (1988) resulting in difficulties for curators to classify *D. heermanni* below the species level.

Given the complexity of the area that *D. heermanni* inhabits and high levels of endemism, it is surprising that my study did not find more diversity within the species (Grinnell 1922; CDFG 2003; Davis et al. 2008; Kuchta et al. 2009). This lack of diversity could be the result of the young evolutionary age of *D. heermanni* given that the recent divergence between *D. heermanni* and *D. panamintinus* (Hafner et al. 2007), approximately a million years after the Coast Ranges formed (Kuchta et al. 2009). Regardless of the cause, there is a general lack of diversity within *D. heermanni*.

Dipodomys heermanni are solitary mammals with male home ranges having some degree of overlap with other males and females during mating season (Tappe 1941; Shier and Yoerg 1999; Shier and Randall 2004, 2007). Males have larger ranges, averaging 0.11 ha, while females have smaller home ranges, averaging 0.04 ha (Shier and Randall 2004, 2007). While the dispersal distance for *D. heermanni* is unknown, relatives of *D. heermanni* have small dispersal distances (median dispersal of 9-34 m for *D. stephensi*; median dispersal distance of 25-62 m for *D. merriami* (Jones 1989; Price et al. 1994)). Even if the dispersal distances of *D. heermanni* are similar, they may still be sufficient to facilitate gene flow across the geographic distribution of the species.

State and national agencies often protect flora and fauna based on historic classifications that may not reflect unique lineages in need of conservation. In fact, recent mammalian intraspecific studies using genetic and other data have sometimes demonstrated a disconnect between classification and phylogeographic relationships (e.g., Andersen and Light 2012; Miller and Jolley-Rogers 2014; Fennessy et al. 2016; Light et al. 2016; Veron and Goodman 2018). Rigorous analyses, including genetic and morphological analyses, can be useful in assessing species and population limits, identifying distinct groups, and redefining taxonomic classifications so that management policies and practices can be put in place to preserve the greatest biodiversity. In the case of *D. heermanni*, a better understanding of intraspecific taxonomy is needed to help state and federal agencies work towards the preservation of the greatest biodiversity. Currently protection has only been offered to one subspecies, *D. h. morroensis*. However, Appendix C of the State Wildlife Action Plan lists five additional subspecies as Species of Special Concern: *D. h. arenae*, *D. h. berkeleyensis*, *D. h. dixoni*, *D. h. goldmani*, and *D. h. heermanni* (CDFW 2016). My results indicate that subspecific designations within *D. heermanni* may not be warranted, and that this species has relatively low genetic diversity across the entirety of its range. Given the low genetic diversity and the importance of kangaroo rats as seed dispersers and ecosystem engineers, influencing distributions of fungi, plants, and animals through their mound building and caching, it would be advantageous for further studies to analyze the abundance of *D. heermann*i across its range and work to preserve the entirety of the species and what is left of its native habitat (Hudson 1958; Kelt 1988; Hastings et al. 2007; Cosentino et al. 2014). Given the apparent lack of genetically or morphologically distinct groups, introductions of *D. heermanni* individuals to areas where *D. heermanni* populations are low (e.g., *D. h. morroensis* and *D. h. berkeleyensis* ranges) could help to restore ecological function.

REFERENCES

ADAMS, D. C., M. L. COLLYER, A. KALIONTZOPOUPOU, AND E. SHERRATT. 2017. Geomorph: Software for geometric morphometric analyses. R package version 3.0.5. <https://cran.r-project.org/package=geomorph>.

ADAMS, D. C., F. J. ROHLF, AND D. E. SLICE. 2004. Geometric morphometrics: Ten years of progress following the 'revolution.' Italian Journal of Zoology 71:5–16.

ADAMS, D. C., F. J. ROHLF, AND D. E. SLICE. 2013. A field comes of age: Geometric morphometrics in the 21st century. Hystrix, The Italian Journal of Mammalogy 24:7–14.

ALEXANDER, L. F., AND B. R. RIDDLE. 2005. Phylogentics of the New World rodent family Heteromyidae. Journal of Mammalogy 86:366–379.

ÁLVAREZ-CASTAÑEDA, S. T., W. Z. LIDICKER, AND E. RIOS. 2009. Revision of the *Dipodomys merriami* complex in the Baja California Peninsula, Mexico. Journal of Mammalogy 90:992–1008.

ANDERSEN, J. J., AND J. E. LIGHT. 2012. Phylogeography and subspecies revision of the hispid pocket mouse, *Chaetodipus hispidus* (Rodentia: Heteromyidae). Journal of Mammalogy 93:1195–1215.

BAUMGARDNER, G. D., AND M. L. KENNEDY. 1994. Patterns of interspecific morphometric variation in kangaroo rats (Genus *Dipodomys*). Journal of Mammalogy 75:203–211.

BENSASSON, D., D. ZHAND, D. HARTL, AND G. HEWITT. 2001. Mitochondrial pseudogenes: ecolution's misplaced witnesses. Trends in Ecology & Evolution 16:314–321.

BERGSTEN, J., A. N. NILSSON, AND F. RONQUIST. 2013. Bayesian tests of topology hypotheses with an example from diving beetles. Systematic Biology 62:660–673.

BOULWARE, J. T. 1943. Two new subspecies of kangaroo rats (genus *Dipodomys*) from southern California. University of California Publications in Zoology 46:391–396.

BRABY, M. F., R. EASTWOOD, AND N. MURRAY. 2012. The subspecies concept in butterflies: Has its application in taxonomy and conservation biology outlived its usefulness? Biological Journal of the Linnean Society 106:699–716.

BRADLEY, R. D., AND R. J. BAKER. 2001. A test of the genetic species concept: cytochrome -*b* sequences and mammals. Journal of Mammalogy 82:960–973.

BRENO, M., H. LEIRS, S. VAN DONGEN, AND E. R. DUMONT. 2011. Traditional and geometric morphometrics for studying skull morphology during growth in *Mastomys natalensis* (Rodentia:Muridae). Journal of Mammalogy 92:1395–1406.

BROWN, D. M. ET AL. 2007. Extensive population genetic structure in the giraffe. BMC Biology 5:1–13.

CALSBEEK, R., J. N. THOMPSON, AND J. E. RICHARDSON. 2003. Patterns of molecular evolution and diversification in a biodiversity hotspot: The California Floristic Province. Molecular Ecology 12:1021–1029.

CARDINI, A., AND P. O'HIGGINS. 2004. Patterns of morphological evolution in *Marmota* (Rodentia, Sciuridae): geometric morphometrics of the cranium in the context of marmot phylogeny, ecology and conservation. Biol J Linn Soc 82:385–407.

CARRASCO, M. A. 2000. Species discimination and morphological relationships of kangaroo rats (*Dipodomys*) based on their dentition. Journal of Mammalogy 81:107–122.

CDFG (CALIFORNIA DEPARTMENT OF FISH AND GAME). 2003. Atlas of the Biodiversity of California. Unites States of America.

CDFW. 2016. California State Wildlife Action Plan.

<https://www.wildlife.ca.gov/SWAP/Final>.

CESA. 1971. California Endangered Species Act [of 1971, as amended], Fish and Game Code Section 2050-2069. <http://www.leginfo.ca.gov/cgi-bin/calawquery?codesection=fgc&codebody=&hits=20>.

Congdon, J., and A. Roest. 1975. Status of the endangered Morro Bay kangaroo rat. Journal of Mammalogy 56:679–683.

Le Conte, J. L. 1853. [Remarks on the genus *Dipodomys*]. Proceedings of the Academy of Natural Sciences of Philadelphia 6:224–225.

Cordeiro-Estrela, P., M. Baylac, C. Denys, and J. Marinho-Filho. 2006. Interspecific patterns of skull variation between sympatric Brazilian vesper mice: geometric morphometrics assessment. Journal of Mammalogy 87:1270–1279.

Cosentino, B. J., R. L. Schooley, B. T. Bestelmeyer, J. F. Kelly, and J. M. Coffman. 2014. Constraints and time lags for recovery of a keystone species (*Dipodomys spectabilis*) after landscape restoration. Landscape Ecology 29:665–675.

Davis, B. W., G. Li, and W. J. Murphy. 2010. Supermatrix and species tree methods resolve phylogenetic relationships within the big cats, *Panthera* (Carnivora: Felidae). Molecular Phylogenetics and Evolution 56:64–76.

Davis, E. B., M. S. Koo, C. Conroy, J. L. Patton, and C. Moritz. 2008. The California hotspots project: identifying regions of rapid diversification of mammals. Molecular Ecology 17:120–138.

Dryden, I. L. 2017. shapes: statistical shape analysis. R package version 1.2.3. <https://cran.r-project.org/package=shapes>.

Eizirik, E., K. Jae-Heup, M. Menotti-Raymond, P. G. Crawshaw, S. J. O'Brien, and W. E.

JOHNSON. 2001. Phylogeography, population history and conservation genetics of jaguars (*Panthera onca*, Mammalia, Felidae). Molecular Ecology 10:65–79.

ESA. 1973. U.S. Endangered Species Act of 1973, as amended, Pub. L. No. 93-205, 87 Stat. 884 (Dec. 28, 1973). <http://www.fws.gov/endangered/esalibrary/%0Apdf/ESAall.pdf.>.

FASHING, N. J. 1973. Implications of karyotypic variation in the kangaroo rat, *Dipodomys heermanni*. Journal of Mammalogy 54:1018–1020.

FENNESSY, J. ET AL. 2016. Multi-locus analyses reveal four giraffe species instead of one. Current Biology 26:2543–2549.

FERNÁNDEZ, J. A., F. A. CERVANTES, AND M. S. HAFNER. 2012. Molecular systematics and biogeography of the Mexican endemic kangaroo rat, *Dipodomys phillipsii* (Rodentia: Heteromyidae). Journal of Mammalogy 93:560–571.

FITCH, H. S. 1948. Habits and economic relationships of the Tulare kangaroo rat. Journal of Mammalogy 29:5–35.

FRALEY, C., AND A. E. RAFTERY. 2003. Enhancing model-based clustering, density estimation, and discriminant analysis software: MCLUST. Journal of Classification 20:263–286.

GARNETT, S. T., AND L. CHRISTIDIS. 2017. Taxonomy anarchy hampers conservation. Nature 546:25–27.

GILBERT, M. T. P., H. J. BANDELT, M. HOFREITER, AND I. BARNES. 2005. Assessing ancient DNA studies. Trends in Ecology and Evolution 20:541–544.

GIPPOLITI, S., AND G. AMORI. 2007. The problem of subspecies and biased taxonomy in conservation lists: The case of mammals. Folia Zoologica 56:113–117.

GOOD, S. V, D. F. WILLIAMS, K. RALLS, R. C. FLEISCHER, AND R. C. FLEISCHER3. 1997. Population structure of *Dipodomys ingens* (Heteromyidae): the role of spatial heterogeneity in maintaining genetic diversity. Evolution 51:1296–1310.

GRINNELL, J. 1919a. Four new kangaroo rats from west-central California. Proceedings of Biological Sciences of Washington 32:203–206.

GRINNELL, J. 1919b. Five new five-toed kangaroo rats from California. University of California Publications in Zoology 21:43–47.

GRINNELL, J. 1922. A Geographic Study of the Kangaroo Rats of California. University of California Publications in Zoology.

GRINNELL, J., AND J. M. LINSDALE. 1929. A new kangaroo rat from the upper Sacramento Valley, California. University of California Press.

HAFNER, J. C. ET AL. 2007. Basal clades and molecular systematics of Heteromyid rodents. Journal of Mammalogy 88:1129–1145.

HALL, E. 1981. The mammals of North America. Pp. 572–579 in. 2nd edition. John Wiley and Sons, New York.

HANFLING, B., B. HELLEMANS, F. A. M. VOLCKAERT, AND G. R. CARVALHO. 2002. Late glacial history of the cold-adapted freshwater fish Cottus gobio, revealed by microsatellites. Molecular Ecology 11:1717–1729.

HASTINGS, A. ET AL. 2007. Ecosystem engineering in space and time. Ecology Letters 10:153–164.

HAUSDORF, B., H. WILKENS, AND U. STRECKER. 2011. Population genetic patterns revealed by microsatellite data challenge the mitochondrial DNA based taxonomy of *Astyanax* in Mexico (Characidae, Teleostei). Molecular Phylogenetics and Evolution 60:89–97.

HERRNSTADT, C. ET AL. 1999. A novel mitochondrial DNA-like sequence in the human nuclear genome. Genomics 60:67–77.

HUDSON, R. G. 1958. The ecology of the Merriam kangaroo rat (*Dipodomys merriami* Mearns) on the grazing lands of southern Arizona. Ecological Society of America 28:111–127.

JOHNSON, W. E., AND R. K. SELANDER. 1971. Protein variation and systematics in kangaroo rats (Genus *Dipodomys*). Systematic Zoology 20:377–405.

JONES, W. T. 1989. Dispersal sitance and the range of nightly movements in Merriam's kangaroo rats. Journal of Mammalogy 70:27–34.

KASS, R. E., AND A. E. RAFTERY. 1995. Bayes factors. Journal of American Statistical Association 90:773–795.

KELT, D. A. 1988. *Dipodomys heermanni*. Mammalian Species:1–7.

KIM, J.-H. ET AL. 2006. Evolutionary analysis of a large mtDNA tanslocation (*numt*) into the nuclear genome of the *Panthera* genus species. Gene 366:292–302.

KOCHER, T. D. ET AL. 1989. Dynamics of mitochondrial DNA evolution in animals: amplification and sequencing with conserved primers. Proceedings of the National Academy of Sciences 86:6196–6200.

KOFRON, C. P., AND F. X. VILLABLANCA. 2016. Decline of the Endangered Morro Bay kangaroo rat in California. Journal of Fish and Wildlife Management 7:237–254.

KUBIAK, B. B., E. E. GUTIÉRREZ, D. GALIANO, R. MAESTRI, AND T. R. O. D. FREITAS. 2017. Can niche modeling and geometric morphometrics document competitive exclusion in a pair of subterranean rodents (Genus *Ctenomys*) with tiny parapatric distributions? Scientific Reports 7:1–13.

KUCHTA, S. R., D. S. PARKS, AND D. B. WAKE. 2009. Pronounced phylogeographic structure on a small spatial scale: geomorphological evolution and lineage history in the salamander ring species *Ensatina eschscholtzii* in central coastal California. Molecular Phylogenetics and

Evolution 5:240–255.

LANFEAR, R., B. CALCOTT, S. Y. W. HO, AND S. GUINDON. 2012. PartitionFinder: Combined selection of partitioning schemes and substitution models for phylogenetic analyses. Molecular Biology and Evolution 29:1695–1701.

LAWING, A. M., AND P. D. POLLY. 2010. Geometric morphometrics: Recent applications to the study of evolution and development. Journal of Zoology 280:1–7.

LEIGH, J., AND D. BRYANT. 2015. PopART: Full-feature software for haplotype network construction. Methods in Ecology and Evolution 6:1110–1116.

LIDICKER, W. Z. J. 1960. An analysis of intraspecific variation in the kangaroo rat *Dipodomys merriami*. University of California Publications in Zoology 67:125–217.

LIDICKER, W. Z. J. 1962. The nature of subspecies boundaries in a desert rodent and its implications for subspecies taxonomy. Systematic Zoology 11:160–171.

LIGHT, J. E., M. O. OSTROFF, AND D. J. HAFNER. 2016. Phylogeographic assessment of the northern pygmy mouse, *Baiomys taylori*. Journal of Mammalogy 97:1081–1094.

MALANEY, J. L., J. R. DEMBOSKI, AND J. A. COOK. 2017. Integrative species delimitation of the widespread North American jumping mice (Zapodinae). Molecular Phylogenetics and Evolution 114:137–152.

MATOCQ, M. D., AND F. X. VILLABLANCA. 2001. Low genetic diversity in an endangered species: Recent or historic pattern? Biological Conservation 98:61–68.

MERRIAM, C. H. 1894. Preliminary description of eleven new kangaroo rats of the genera *Dipodomys* and *Perodipus*. Proceedings of Biological Sciences of Washington 9:109–116.

MERRIAM, C. H. 1904. New and little known kangaroo rats of the genus *Perodipus*. Proceedings of Biological Sciences of Washington 17:139–146.

MERRIAM, C. H. 1907. Descriptions of ten new kangaroo rats. Proceedings of Biological Sciences of Washington 20:75–80.

MILLER, J. T., AND G. JOLLEY-ROGERS. 2014. Correcting the disconnect between phylogenetics and biodiversity informatics. Zootaxa 3754:195–200.

MILLER, M. A., W. PFEIFFER, AND T. SCHWARTZ. 2010. Creating the CIPRES Science Gateway for inference of large phylogenetic trees. Pp. 1–8 in Proceedings of the Gateway. Computing Environments Workshop (GCE). New Orleans, LA.

MORITZ, C. 1994. Defining "Evolutionarily Significant Units" for conservation. Trends in Ecology & Evolution 9:373–375.

MUSIANI, M. ET AL. 2007. Differentiation of tundra/taiga and boreal coniferous forest wolves: Genetics, coat colour and association with migratory caribou. Molecular Ecology 16:4149–4170.

PATTON, J. L., AND C. J. CONROY. 2017. The conundrum of subspecies: morphological diversity among desert populations of the California vole (*Microtus californicus*, Cricetidae). Journal of Mammalogy 98:1010–1026.

PATTON, J. L., H. MACARTHUR, AND S. Y. YANG. 1976. Systematic relationships of the four-toed populations of *Dipodomys heermanni*. Journal of Mammalogy 57:159–163.

PONTIUS, J. U. ET AL. 2007. Initial sequence and comparative analysis of the cat genome. Genome Resource 17:1675–1689.

POSADA, D. 2008. jModelTest: phylogenetic model averaging. Molecular Biology and Evolution 7:1253–6.

PRICE, M. V, P. A. KELLY, AND R. L. GOLDINGAY. 1994. Distances moved by Stephens ' kangaroo rat (*Dipodomys stephensi* Merriam) and implications for conservation. Journal of

Mammalogy 75:929–939.

PUSCH, C. M., AND L. BACHMANN. 2004. Spiking of contemporary human template DNA with ancient DNA extracts induces mutations under PCR and generates nonauthentic mitochondrial sequences. Molecular Biology and Evolution 21:957–964.

QUINTELA, F. M., R. FORNEL, AND T. R. O. FREITAS. 2016. Geographic variation in skull shape of the water rat *Scapteromys tumidus* (Cricetidae, Sigmodontinae): isolation-by-distance plus environmental and geographic barrier effects? Anais da Academia Brasileira de Ciencias 88:451–466.

RAMBAUT, A. 1996. Se-Al, sequence alignment editor. Version 2.01all.

REIS, S. F. DOS, L. C. DUARTE, L. R. MONTEIRO, AND F. J. VON ZUBEN. 2002. Geographic variation in cranial morphology in *Thrichomys apereoides* (Rodentia:Echimyidae). II. Geographic units, morphological discontinuities, and sampling gaps. Journal of Mammalogy 83:345–353.

RICHLY, E., AND D. LEISTER. 2004. NUMTs in sequenced eukaryotic genomes. Molecular Biology and Evolution 21:1081–1084.

RISSER, R. 1976. The taxonomy of *Dipodomys heermanni* and *Dipodomys agilis* in central California. Cal Poly State University, San Luis Obispo.

RITZ, L. R., M.-L. GLOWATZKI-MULLIS, D. E. MACHUGH, AND C. GAILLARD. 2000. Phylogenetic analysis of the tribe Bovini using microsatellites. Animal Genetics 31:178–185.

ROHLF, F. J. 2015. The tps series of software. Hystrix 26.

RONQUIST, F., AND J. P. HUELSENBEACK. 2003. MrBayes 3: Phylogenetic inference under mixed models. Bioinformatics 19:1572–1574.

ROURE, B., D. BAURAIN, AND H. PHILIPPE. 2012. Impact of missing data on phylogenies inferred from empirical phylogenomic data sets. Molecular Biology and Evolution 30:197–214.

RUIZ-GARCÍA, M., M. PINEDO-CASTRO, AND J. M. SHOSTELL. 2014. How many genera and species of woolly monkeys (Atelidae, Platyrrhine, Primates) are there? The first molecular analysis of *Lagothrix flavicauda*, an endemic Peruvian primate species. Molecular Phylogenetics and Evolution 79:179–198.

SACKETT, L. ET AL. 2014. Evidence for two subspecies of Gunnison's prairie dogs (*Cynomys gunnisoni*), and the general importance of the subspecies concept. Biological Conservation 174:1–11.

SCHMIEDER, D. A., H. A. BENÍTEZ, I. M. BORISSOV, AND C. FRUCIANO. 2016. Bat species comparisons based on external morphology: a test of traditional versus geometric morphometric approaches. PLoS ONE 10:1–13.

SCRUCCA, L., M. FOB, T. B. MURPHY, AND A. E. RAFTERY. 2016. mclust 5: clustering, classification and density estimation using Gaussian finite mixture models. The R Journal 8/1:205–233.

SFPUC. 2011. Alameda Habitat Conservation Plan. *San Francisco Water Power Sewer*. <http://sfwater.org/index.aspx?page=412>.

SHIER, D. M., AND J. A. RANDALL. 2004. Spacing as a predictor of social organization in kangaroo rats (*Dipodomys heermanni arenae*). Journal of Mammalogy 85:1002–1008.

SHIER, D. M., AND J. A. RANDALL. 2007. Use of different signaling modalities to communicate status by dominant and subordinate Heermann's kangaroo rats (*Dipodomys heermanni*). Behavioral Ecology and Sociobiology 61:1023–1032.

SHIER, D. M., AND S. I. YOERG. 1999. What Footdrumming Signals in Kangaroo Rats (*Dipodomys heermanni*). Journal of Comparative Psychology 113:66–73.

SMITH, M. F., AND J. L. PATTON. 1991. Variation in the mitochondrial cytochrome b sequence in natural populations in South American akodontine rodents (Muridae: Sigmodontinae). Molecular Biology and Evolution 8:85–103.

SORENSON, M. D., J. C. AST, D. E. DIMCHEFF, T. YURI, AND D. P. MINDELL. 1999. Primers for a PCR-based approach to mitochondrial genome sequencing in birds and other vertebrates. Molecular Phylogenetics and Evolution 12:105–114.

SORENSON, M. D., AND T. W. QUINN. 1998. Numts : A challenge for avian systematics and population biology. American Ornithological Society 115:214–221.

STANFORD, C. B. 2001. The subspecies concept in primatology: the case of mountain gorillas. Primates 42:309–318.

STOCK, A. D. 1974. Chromosome evolution in genus *Dipodomys* and its taxonomic and phylogenetic implications. Journal of Mammalogy 55:505–526.

SWOFFORD, D. L. 2003. PAUP*: phylogenetic analysis using parsimony (*and other methods). Version 4. Sinauer Associates, Inc., Sunderland, Massachusetts.

TAPPE, D. T. 1941. Natural history of the Tulare kangaroo rat. Journal of Mammalogy 22:117–148.

TEAM, R. C. 2017. R: A language and environment for statistical computing. R Foundation for Statistical Computing, Vienna, Austria. <https://www.r-project.org/>.

TEMPLETON, A. R., K. A. CRANDALL, AND C. F. SING. 1992. A cladistic analysis of phenotypic associations with haplotypes inferred from restriction endonuclease mapping and DNA sequence data. III. Cladogram estimation. Genetics 132:619–633.

THALMANN, O., J. HEBLER, H. N. POINAR, S. PÄÄBO, AND L. VIGILANT. 2004. Unreliable mtDNA data due to nuclear insertions: a cautionary tale from analysis of humans and other great apes. Molecular Ecology 13:321–335.

THOMAS, W. K., S. PAABO, F. X. VILLABLANCA, AND A. C. WILSON. 1990. Spatial and temporal continuity of kangaroo rat populations shown by sequencing mitochondrial DNA from museum specimens. Journal of Molecular Evolution 31:101–112.

USFWS. 1970. Appendix D, United States list of Endangered species. Federal Register 35:16047–16048.

USFWS. 1999. Morro Bay kangaroo rat draft revised recovery plan in USFWS, editor.

USFWS. 2002. Draft recovery plan for chaparral and scrub community species east of San Francisco Bay, California. Region 1, Portland, OR.

USFWS. 2017. Berkeley kangaroo rat (*Dipodomys heermanni berkeleyensis*). *Environmental Conservation Online System*. <http://ecos.fws.gov/ecp0/profile/speciesProfile?spcode=A0GY>.

VENABLES, W. N., AND B. D. RIPLEY. 2002. Modern Applied Statistics with S. Springer, New York.

VERON, G., AND S. GOODMAN. 2018. One or two species of the rare Malagasy carnivoran *Eupleres* (Eupleridae)? New insights from molecular data. Mammalia 82:107–112.

VILLABLANCA, F. 2009. Protocol surveys for the Morro Bay kangaroo rat (Year 1) 2008.

VILLABLANCA, F. X. 1994. Evolutionary analysis: spatial and temporal aspects of populations revealed by mitochondrial DNA. Pp. 31–58 in Herramann, B,. Hummel, S. (Eds.), Ancient DNA: Recovery and Analysis of Genetic Material from Paleontological, Archaeological, Museum, Medical, and Forensic Specimens. Springer-Verlag, New York.

VILLABLANCA, F. X. 2007. Morphological and genetic divergence of Morro Bay kangaroo rats:Agreement #P0485102 and #S0685103, CDFW.

WIENS, J. J., AND D. S. MOEN. 2008. Missing data and the accuracy of Bayesian phylogenetics. Journal of Systematics and Evolution 46:307–314.

WIENS, J. J., AND M. C. MORRILL. 2011. Missing data in phylogenetic analysis: Reconciling results from simulations and empirical data. Systematic Biology 60:719–731.

WILLERSLEV, E., AND A. COOPER. 2005. Ancient DNA. Proceedings of the Royal Society B: Biological Sciences 272:3–16.

WILSON, D. E., AND D. M. REEDER. 2005. Mammal species of the world: a taxonomic and geographic reference. Johns Hopkins University Press, Baltimore, Maryland.

WILSON, E. O., AND W. L. BROWN. 1953. The subspecies concept and its taxonomic application. Society of Systematic Biologists 2:97–111.

XIE, W., P. O. LEWIS, Y. FAN, L. KUO, AND M. H. CHEN. 2011. Improving marginal likelihood estimation for bayesian phylogenetic model selection. Systematic Biology 60:150–160.

YAZDI, T., AND D. ADRIAENS. 2011. Patterns of skull shape variation in *Meriones persicus* (Rodentia: Muridae) in relation to geoclimatical conditions. Iranian Journal of Animal Biosystematic 7:129–142.

ZHANG, D., AND G. M. HEWITT. 1996. Nuclear integrations: challenges for mitochondrial DNA markers. Trends in Ecology & Evolution 11:247–251.

APPENDIX A

Heermann's kangaroo rat (*Dipodomys heermanni*) specimens examined with molecular data. All specimens are from California. Abbreviations are as follows: The Museum of Vertebrate Zoology at Berkeley (MVZ), Natural History Museum of Los Angeles (LACM), Sam Noble Oklahoma Museum of Natural History (OMNH), Museum of Southwestern Biology (MSB), New Mexico Museum of Natural History and Science (NMMNH), Moore Laboratory of Zoology, Occidental College (MLZ), University of Nevada, Las Vegas (LVT), and specimens captured and released by Joseph DiDonato (BE). GenBank numbers are pending. Those specimens lacking GenBank numbers entirely were processed in the laboratory but failed to successfully amplify and/or sequence.

Gen Bank *Cytb*	**Gen Bank *ND2***	**Gen Bank *Dloop***	**Museum Number**	**Subspecies or Species Name**	**Locality (latitude, longitude)**
Frozen Tissue Specimens					
X	X	-	MVZ 179780	*arenae*	San Luis Obispo Co.: Nipomo Mesa, 0.5 mi W Hwy. 1, 0.5 mi SSE White Lake (35.058832, -120.601075)
X	X	-	MVZ 223091	*berkeleyensis*	Alameda Co.: Haera property, Patterson Pass (37.71978, -121.58631)
X	X	X	BE050005	*berkeleyensis*	Alameda Co.: Haera Widlife Conservation Bank, 1.71 km NW PG&E Substation, Patterson Pass Road (37.7197233333333, -121.586446666667)
X	X	X	BE050006	*berkeleyensis*	Alameda Co.: Haera Widlife Conservation Bank, 1.71 km NW PG&E Substation, Patterson Pass Road (37.7197233333333, -121.586446666667)

Continued

Gen Bank *Cytb*	Gen Bank *ND2*	Gen Bank *Dloop*	Museum Number	Subspecies or Species Name	Locality (latitude, longitude)
X	X	X	BE050009	*berkeleyensis*	Alameda Co.: Haera Widlife Conservation Bank, 1.71 km NW PG&E Substation, Patterson Pass Road (37.7199016666667, -121.585236666667)
X	X	-	MVZ 216714	*berkeleyensis*	Alameda Co.: 4 1/2 mi S Del Valle Dam, Ohlone Regional Wilderness, Mendenhall Springs (37.5510535898, -121.7411088681)
X	X	-	BE050001	*berkeleyensis*	Alameda Co.: Ohlone-West Conservation Bank, Livermore (37.55605, -121.763495)
X	-	-	BE050002	*berkeleyensis*	Alameda Co.: Ohlone-West Conservation Bank, Livermore (37.5564416666667, -121.760265)
X	X	X	BE050004	*berkeleyensis*	Alameda Co.: Ohlone-West Conservation Bank, Livermore (37.55402, -121.757375)
X	X	X	BE050007	*berkeleyensis*	Alameda Co.: Ohlone-West Conservation Bank, Livermore (37.5561716666667, -121.761728333333)
X	X	-	MVZ 216722	*berkeleyensis*	Alameda Co.: Ohlone Preserve (SE 1/4 sect. Sect. 28) (37.7916, -121.7569387)
X	X	X	MVZ 207393	*dixoni*	Mariposa Co.: 1.4 mi W Mt. Bullion (37.50331, -120.06969)
X	X	X	MVZ 207404	*dixoni*	Mariposa Co.: Hunter Valley Mt. (37.65594, -120.22132)
-	X	X	MVZ 207405	*dixoni*	Mariposa Co.: Hunter Valley Mt. (37.65594, -120.22132)
X	X	X	MVZ 207399	*dixoni*	Merced Co.: Kelsey Ranch, 5.2 mi E Snelling (37.54598, -120.35863)
X	X	X	MVZ 207400	*dixoni*	Merced Co.: Kelsey Ranch, 5.2 mi E Snelling (37.54598, -120.35863)
X	X	X	MVZ 182332	*goldmani*	Monterey Co.: Dunes E bank Salinas River, 1.2 mi N and 2.1 mi E Greenfield (36.337722, -121.202646)

Continued

Gen Bank *Cytb*	Gen Bank *ND2*	Gen Bank *Dloop*	Museum Number	Subspecies or Species Name	Locality (latitude, longitude)
X	X	-	MVZ 182333	*goldmani*	Monterey Co.: Dunes E bank Salinas River, 1.2 mi N and 2.1 mi E Greenfield (36.337722, -121.202646)
X	X	X	MVZ 195192	*goldmani*	Monterey Co.: Shirttail Canyon, 4.8 mi E Soledad (36.433446, -121.227359)
X	X	-	MVZ 195193	*goldmani*	Monterey Co.: 5.2 mi NE King City (36.270044, -121.06419)
X	X	X	MVZ 195196	*goldmani*	San Benito Co.: 9.1 mi NE King City (Monterey Co.) (36.282766, -120.987678)
-	-	-	MVZ 228908	*jolonensis*	Monterey Co.: Bayonet Course, Camp Roberts (35.803002, -120.744812)
X	X	X	MVZ 181316	*jolonensis*	San Luis Obispo Co.: 0.2 mi S Hwy. 1 and 0.3 mi W Railroad Tracks, Callender Substation, Nipomo Mesa (35.76924, -120.79965)
X	X	-	MVZ 182343	*jolonensis*	San Luis Obispo Co.: 2.3 mi E and 4.9 mi S Shandon (35.581383, -120.327076)
X	-	-	MVZ 228909	*jolonensis*	San Luis Obispo Co.: Camp Roberts Military Reservation (35.77, -120.79)
X	-	-	MVZ 228907	*jolonensis*	San Luis Obispo Co.: Near intersection of Bee Rock Rd. and Tower Rd., Camp Roberts (35.785482, -120.799179)
X	X	X	MVZ 198627	*swarthi*	Kern Co.: Temblor Range summit on Hwy. 58 (35.35564, -119.82853)
X	X	X	MVZ 196746	*swarthi*	San Luis Obispo Co.: 0.4 mi S Wells Ranch, Caliente Range (35.04427, -119.89468)
X	X	X	MVZ 181313	*swarthi*	San Luis Obispo Co.: 1.1 mi W and 0.5 mi N Temblor Peak (35.070583, -119.509332)
X	X	X	MVZ 181317	*swarthi*	San Luis Obispo Co.: 1.1 mi W and 0.5 mi N Temblor Peak (35.070583, -119.509332)
X	X	-	MVZ 196748	*swarthi*	San Luis Obispo Co.: 13.3 mi NW (by road) New Cuyama (35.04427, -119.89468)

Continued

Gen Bank *Cytb*	Gen Bank *ND2*	Gen Bank *Dloop*	Museum Number	Subspecies or Species Name	Locality (latitude, longitude)
X	X	X	MVZ 195959	*swarthi*	San Luis Obispo Co.: Beam Flat, Elkhorn Hills (35.0191166667, -119.4924833333)
-	-	-	MVZ 228893	*swarthi*	San Luis Obispo Co.: Swain Pasture, Carrizo Plain National (35.082688, -119.668717)
X	X	X	MVZ 223154	*tularensis*	San Joaquin Co.: 1 mi ESE Castle Rock off of Corral Hollow Rd. (37.63175, -121.4756666667)
X	X	X	MVZ 223155	*tularensis*	San Joaquin Co.: 1 mi ESE Castle Rock off of Corral Hollow Rd. (37.63175, -121.4756666667)
Ancient Specimens					
X	-	X	LACM 32106	*arenae*	San Luis Obispo Co.: Nipoino, 13 mi E; Cuyuma River Gorge; Hwy 166, 2 mi W, from Pine Cyn R S (35.0214654, -120.221869)
X	-	X	MVZ 84841	*arenae*	Santa Barbara Co.: C.A. Davis Ranch, 1.75 mi N Lompoc (34.633833, -120.4436667)
X	-	X	MVZ 77311	*berkeleyensis*	Alameda Co.: 7 mi E and 8 mi S Livermore (37.56619, -121.63853)
X	-	X	MVZ 95168	*berkeleyensis*	Alameda Co.: Calaveras Dam (37.4925, -121.8196)
-	-	-	MVZ 28770	*berkeleyensis*	Alameda Co.: Dwight Way Hill, Berkeley (37.8677891, -122.2367154)
X	-	X	MVZ 69961	*berkeleyensis*	Contra Costa Co.: W side Mount Diablo (37.8816953, -121.9130424)
X	-	X	MVZ 69962	*berkeleyensis*	Contra Costa Co.: W side Mount Diablo (37.8816953, -121.9130424)
-	-	X	MVZ 21843	*dixoni*	Merced Co.: Snelling (37.52078, -120.43822)
-	-	X	MVZ 21846	*dixoni*	Merced Co.: 5 mi N Snelling (37.57188, -120.4247)
X	-	X	MVZ 21850	*dixoni*	Merced Co.: 5 mi N Snelling (37.57188, -120.4247)

Continued

Gen Bank *Cytb*	Gen Bank *ND2*	Gen Bank *Dloop*	Museum Number	Subspecies or Species Name	Locality (latitude, longitude)
X	-	X	MVZ 22541	*dixoni*	Merced Co.: 1.5 mi S Merced Falls (37.49539, -120.308)
X	-	X	MVZ 46420	*dixoni*	Merced Co.: Delhi (37.43266, -120.777351)
X	-	X	MVZ 23613	*dixoni*	Stanislaus Co.: La Grange (37.6661, -120.469857)
X	-	X	MVZ 55059	*goldmani*	Fresno Co.: Warthan Creek, 4.5 mi SE Priest Valley (36.1576, -120.6097)
X	-	X	MVZ 101745	*goldmani*	Monterey Co.: Chualar Canyon, 5 mi from (East) Chualar (36.599043, -121.433393)
X	-	X	MVZ 108323	*goldmani*	Monterey Co.: E side Salinas River, 5 mi W Salinas (36.677043, -121.736999)
X	-	X	MVZ 140086	*goldmani*	Monterey Co.: Hastings Natural History Reservation (36.37851365, -121.5568207)
X	-	X	MVZ 108364	*goldmani*	Monterey Co.: Lewis Creek (36.2379, -120.9887)
X	-	X	MVZ 108352	*goldmani*	Monterey Co.: Metz, Salinas Valley (36.355297, -121.207773)
X	-	X	MVZ 108316	*goldmani*	Monterey Co.: Monterey (36.59962, -121.897474)
X	-	X	MVZ 108340	*goldmani*	Monterey Co.: mouth of Vaqueros Canyon (36.26527, -121.336082)
X	-	X	MVZ 3482	*goldmani*	Monterey Co.: Sandhills, 2 mi S mouth Salinas River (36.72202, -121.79811)
X	-	X	MVZ 28506	*goldmani*	San Benito Co.: 1 mi N Cook Post Office, Bear Valley (36.547167, -121.1441667)
-	-	-	LACM 88719	*goldmani*	San Benito Co.: 4-1/2 mi S, 3 mi W Hollister, Fremont Peak (36.7905613, -121.4667115)
X	-	X	MVZ 72675	*goldmani*	San Benito Co.: San Benito (36.5082208, -121.0816515)
X	-	X	MVZ 119035	*heermanni*	Amador Co.: Carbondale (38.41003, -121.013288)
X	-	X	MVZ 85254	*heermanni*	Calaveras Co.: 1.5 mi NW Sheepranch (38.2180278, -120.473572)
X	-	X	MVZ 84285	*heermanni*	El Dorado Co.: 7 mi W and 3 mi S Placerville (38.68622, -120.92705)

Continued

Gen Bank *Cytb*	Gen Bank *ND2*	Gen Bank *Dloop*	Museum Number	Subspecies or Species Name	Locality (latitude, longitude)
X	-	X	MVZ 30020	*heermanni*	Mariposa Co.: 1 mi W Coulterville (37.710817, -120.213175)
X	-	X	MVZ 29092	*jolonensis*	Monterey Co.: Jolon (35.97071, -121.173723)
X	-	X	MVZ 190042	*jolonensis*	Monterey Co.: 1.5 mi SW Jolon (35.946683, -121.176576)
X	-	X	MVZ 228908	*jolonensis*	Monterey Co.: Bayonet Course, Camp Roberts (35.803002, -120.744812)
X	-	X	MVZ 122134	*jolonensis*	San Luis Obispo Co.: 3.5 mi SE Cholame (35.695428, -120.252334)
X	-	X	MVZ 125739	*morroensis*	San Luis Obispo Co.: 4 mi S Morro (35.29653, -120.84369)
-	-	-	MVZ 29084	*morroensis*	San Luis Obispo Co.: 4.5 mi S Morro (35.28734, -120.84366)
-	-	-	LACM 48464	*morroensis*	San Luis Obispo Co.: 7.2 mi SW Atascadero (35.41226, -120.75633)
-	-	-	LACM 1781	*morroensis*	San Luis Obispo Co.: Morro (35.3469077, -120.8486777)
X	-	X	MVZ 57112	*swarthi*	Kern Co.: 10 mi NE Taft (35.243833, -119.3288333)
X	-	X	MVZ 138344	*swarthi*	Monterey Co.: Metz, Salinas Valley (36.355297, -121.207773)
X	-	X	LACM 32148	*swarthi*	San Luis Obispo Co.: La Panza Range; Pozo, 6 mi NE (35.36518, -120.3)
-	-	X	MVZ 42247	*swarthi*	San Luis Obispo Co.: 7 mi SE Simmler, Carrizo Plains (35.27959, -119.89931)
-	-	X	LACM 44899	*swarthi*	San Luis Obispo Co.: Carrizo Plain; Soda Lake Road, 8.5 mi N (35.2213452, -119.8575801)
X	-	X	MVZ 46770	*swarthi*	San Luis Obispo Co.: 9 mi W Simmler (35.383299, -120.122876)
X	-	X	LACM 88785	*swarthi*	Santa Barbara Co.: 9 mi N, 25 mi W New Cuyama (35.0784827, -120.1298346)
X	-	X	LACM 88795	*swarthi*	Ventura Co.: 25 mi W Gorman, 1/2 mi E Nettle Springs Camp (34.80362, -119.28258)
-	-	-	LACM 52640	*swarthi*	Ventura Co.:Ojai, S of Meyers Road, W of Oso Road (34.458687, -119.2881606)

Continued

Gen Bank *Cytb*	Gen Bank *ND2*	Gen Bank *Dloop*	Museum Number	Subspecies or Species Name	Locality (latitude, longitude)
X	-	X	MVZ 25171	*tularensis*	Fresno Co.: 1.25 mi S Dunlap (36.723617, -119.11036)
X	-	X	MVZ 107498	*tularensis*	Kern Co.: 2 mi N McKittrick (35.3346666667, -119.623)
X	-	X	MVZ 183779	*tularensis*	Kern Co.: 7.5 mi S, 10.25 mi W Bakersfield (35.2130458, -119.2193935)
X	-	X	MVZ 158793	*tularensis*	Kern Co.: Caliente Creek Wash, 8.3 mi E, 1.4 mi S Edison (35.326, -118.7256667)
-	-	-	MVZ 47491	*tularensis*	Kern Co.: Rose Station (34.9627123, -118.9157426)
X	-	X	LACM 48479	*tularensis*	Kern Co.: Tehachapi, 13 mi SW (34.9948125, -118.2840382)
-	-	-	LACM 3106	*tularensis*	Fresno Co.: Coalinga (36.14, -120.359)
-	-	-	LACM 3662	*tularensis*	Fresno Co.: Mendota, 15 mi S (36.5320464, -120.3815514)
X	-	X	MVZ 198289	*tularensis*	Kings Co.: ca. 12.6 mi SSE Avenal (35.83962, -120.01631)
X	-	X	MVZ 116721	*tularensis*	Madera Co.: San Joaquin Experimental Range (37.090636, -119.721443)
X	-	X	MVZ 14390	*tularensis*	Merced Co.: Los Baños (37.060514, -120.84778)
X	-	X	LACM 38156	*tularensis*	San Benito Co.: Panoche, 4 mi E; Panoche Creek (36.5922343, -120.7638276)
X	-	X	MVZ 72722	*tularensis*	San Benito Co.: Panoche Creek, 2 mi SE Panoche (36.57583, -120.80917)
X	-	-	MVZ 14406	*tularensis*	Tulare Co.: Tipton (36.059519, -119.31074)
X	-	X	MVZ 28488	*tularensis*	Tulare Co.: 2 mi W Earlimart (35.883447, -119.311289)
GenBank Samples					
-	-	AF225926	MVZ 84841	*arenae*	Santa Barbara Co.: C.A. Davis Ranch, 1 3/4 mi N Lompoc (34.633833, -120.4436667)

Continued

Gen Bank *Cytb*	Gen Bank *ND2*	Gen Bank *Dloop*	Museum Number	Subspecies or Species Name	Locality (latitude, longitude)
-	-	AF225928	MVZ 89905	*arenae*	Santa Barbara Co.: C.A. Davis Ranch, 3 1/2 mi NNW Lompoc (34.691, -120.4303333)
-	-	AF225929	MVZ 89906	*arenae*	Santa Barbara Co.: C.A. Davis Ranch, 3.5 mi NNW Lompoc (34.691, -119.569666666667)
-	-	AF225930	MVZ 89907	*arenae*	Santa Barbara Co.: C.A. Davis Ranch, 3.5 mi NNW Lompoc (34.691, -119.569666666667)
-	-	AF225931	MVZ 89908	*arenae*	Santa Barbara Co.: C.A. Davis Ranch, 3.5 mi NNW Lompoc (34.691, -119.569666666667)
-	-	AF225932	MVZ 89909	*arenae*	Santa Barbara Co.: C.A. Davis Ranch, 3.5 mi NNW Lompoc (34.691, -119.569666666667)
-	-	AF225933	MVZ 89910	*arenae*	Santa Barbara Co.: C.A. Davis Ranch, 3.5 mi NNW Lompoc (34.691, -119.569666666667)
-	-	AF225934	2479	*morroensis*	
-	-	AF225935	2486	*morroensis*	
-	-	AF225936	320	*morroensis*	
-	-	AF225937	324	*morroensis*	
-	-	AF225938	1391	*morroensis*	
-	-	AF225939	1579	*morroensis*	
-	-	AF225940	2487	*morroensis*	
-	-	AF225941	366	*morroensis*	
-	-	AF225942	MVZ 29025	*morroensis*	San Luis Obispo Co.: 4.5 mi S Morro (35.28734, -120.84366)
-	-	AF225943	MVZ 29032	*morroensis*	San Luis Obispo Co.: 4.5 mi S Morro (35.28734, -120.84366)
-	-	AF225944	MVZ 29037	*morroensis*	San Luis Obispo Co.: 4.5 mi S Morro (35.28734, -120.84366)

Continued

Gen Bank *Cytb*	Gen Bank *ND2*	Gen Bank *Dloop*	Museum Number	Subspecies or Species Name	Locality (latitude, longitude)
-	-	AF225945	MVZ 29045	*morroensis*	San Luis Obispo Co.: 4.5 mi S Morro (35.28734, -120.84366)
-	-	AF225946	MVZ 29058	*morroensis*	San Luis Obispo Co.: 4.5 mi S Morro (35.28734, -120.84366)
-	-	AF225947	MVZ 29061	*morroensis*	San Luis Obispo Co.: 4 mi S Morro (35.29653, -120.84369)
-	-	AF225948	MVZ 29065	*morroensis*	San Luis Obispo Co.: 4.5 mi S Morro (35.28734, -120.84366)
-	-	AF225949	MVZ 29073	*morroensis*	San Luis Obispo Co.: 4.5 mi S Morro (35.28734, -120.84366)
Frozen Tissue Sequences From James Patton					
X	-	-	MVZ 207394	*dixoni*	Mariposa Co.: 1.4 mi W Mt. Bullion (37.50331, -120.06969)
X	-	-	MVZ 207395	*dixoni*	Mariposa Co.: 1.4 mi W Mt. Bullion (37.50331, -120.06969)
X	-	-	MVZ 207396	*dixoni*	Mariposa Co.: 1.4 mi W Mt. Bullion (37.50331, -120.06969)
X	-	-	MVZ 207406	*dixoni*	Mariposa Co.: Hunter Valley Mt. (37.63996, -120.21697)
X	-	-	MVZ 207405	*dixoni*	Mariposa Co.: Hunter Valley Mt. (37.65594, -120.22132)
X	-	-	MVZ 207398	*dixoni*	Merced Co.: Kelsey Ranch, 5.2 mi NE Snelling (37.54598, -120.35863)
X	-	-	MVZ 207401	*dixoni*	Merced Co.: Kelsey Ranch, 5.2 mi E Snelling (37.54598, -120.35863)
X	-	-	MVZ 207402	*dixoni*	Merced Co.: Kelsey Ranch, 5.2 mi E Snelling (37.54598, -120.35863)
X	-	-	MVZ 207403	*dixoni*	Merced Co.: Kelsey Ranch, 5.2 mi E Snelling (37.54927, -120.34974)
X	-	-	MVZ 195194	*goldmani*	Monterey Co.: 5.2 mi NE King City (36.270044, -121.06419)
X	-	-	MVZ 195195	*goldmani*	Monterey Co.: 5.2 mi NE King City (36.270044, -121.06419)

Continued

Gen Bank *Cytb*	Gen Bank *ND2*	Gen Bank *Dloop*	Museum Number	Subspecies or Species Name	Locality (latitude, longitude)
X	-	-	MVZ 196747	*swarthi*	San Luis Obispo Co.: 0.4 mi S Wells Ranch, Caliente Range (35.04427, -119.89468)
X	-	-	MVZ 198630	*swarthi*	San Luis Obispo Co.: San Diego Creek, Temblor Range (35.33341, -119.84337)
X	-	-	MVZ 198631	*swarthi*	San Luis Obispo Co.: San Diego Creek, Temblor Range (35.33341, -119.84337)
X	-	-	MVZ 198628	*swarthi*	Kern Co.: Temblor Range summit on Hwy. 58 (35.35564, -119.82853)
X	-	-	MVZ 198629	*swarthi*	Kern Co.: Temblor Range summit on Hwy. 58 (35.35564, -119.82853)
X	-	-	MVZ 198289	*tularensis*	Kings Co.: ca. 12.6 mi SSE Avenal (35.83962, -120.01631)
Outgroups					
-	EF156834	**-**	MVZ 153957	*D. agilis*	
-	EF156843	**-**	MLZ 1879	*D. panamintinus*	
DG870429	-	**-**	MLZ 2065	*D. deserti*	
AF173501	-	**-**	OMNH 28957	*D. ordii*	
AF173502	-	**-**	MSB 26206	*D. merriami*	
AY926384	-	**-**	LVT 4672	*D. panamintinus*	
AF173503	-	**-**	MSB 11680	*D. spectabilis*	
-	-	KP059611	LVT NG932	*D. deserti*	
-	-	KP059612	LVT NG933	*D. deserti*	
-	-	KP059831	LVT 7818	*D. merriami*	
-	-	KP059832	LVT 7809	*D. merriami*	

APPENDIX B

Heermann's kangaroo rat (*Dipodomys heermanni*) specimens examined with morphological data. All specimens are from California. Museum abbreviations are as follows: The Museum of Vertebrate Zoology at Berkeley (MVZ) and Natural History Museum of Los Angeles (LACM). Successful imaging of dorsal and ventral cranial views are indicated with an "X". Asterisks by museum numbers indicate type specimens.

Dorsal View	Ventral View	Museum Number	Subspecies Name	Locality (latitude, longitude)
X	X	MVZ 185215	*arenae*	San Luis Obispo Co.: Guadalupe, Unocal Oil Field N of Santa Maria (34.97955, -120.6332)
X	-	MVZ 179780	*arenae*	San Luis Obispo Co.: Nipomo Mesa, 0.5 mi W Hwy. 1, 0.5 mi SSE White Lake (35.058832, -120.601075)
X	X	LACM 32106	*arenae*	San Luis Obispo Co.: Nipoino, 13 mi E; Cuyuma River Gorge; Hwy 166, 2 mi W, from Pine Cyn R S (35.0214654, -120.221869)
X	X	LACM 32135	*arenae*	San Luis Obispo Co.: Nipomo, 24 mi E; Pine Canyon Ranger Station, 5-6 mi E; Gypsum Cyn & Cuyuma R G (35.0274962, -120.2768258)
X	X	MVZ 97319	*arenae*	Santa Barbara Co.: 2.4 mi W Buellton (34.6145, -120.2348333)
X	X	MVZ 84841	*arenae*	Santa Barbara Co.: C.A. Davis Ranch, 1.75 mi N Lompoc (34.633833, -120.4436667)
X	X	MVZ 84840*	*arenae*	Santa Barbara Co.: C.A. Davis Ranch, 1.75 mi N Lompoc (34.633833, -120.4436667)
X	X	MVZ 89911	*arenae*	Santa Barbara Co.: C.A. Davis Ranch, 3.5 mi NNW Lompoc (34.691, -120.4303333)
X	X	LACM 32077	*arenae*	Santa Barbara Co.: Garey, 1 mi N; Cuyuma River & Sisquoc River Junction (34.8904259, -120.315452)

Continued

Dorsal View	Ventral View	Museum Number	Subspecies Name	Locality (latitude, longitude)
X	X	LACM 38430	*arenae*	Santa Barbara Co.: Lompoc, 2 mi NNW (34.6817805, -120.477762)
X	X	MVZ 182142	*berkeleyensis*	Alameda Co.: 12 mi SW Tracy (37.594971, -121.576263)
X	X	MVZ 102384	*berkeleyensis*	Alameda Co.: 7 mi SE Livermore (37.6259, -121.6756)
X	X	MVZ 77311	*berkeleyensis*	Alameda Co.: 7 mi E and 8 mi S Livermore (37.56619, -121.63853)
X	X	MVZ 95168	*berkeleyensis*	Alameda Co.: Calaveras Dam (37.4925, -121.8196)
X	X	MVZ 102385	*berkeleyensis*	Alameda Co.: Corral Hollow, 2 mi E Tesla (37.6365633, -121.5585082)
X	X	MVZ 128631	*berkeleyensis*	Alameda Co.: Corral Hollow, 2 mi W Alameda--San Joaquin Co. boundary (37.6415333, -121.5903634)
X	X	MVZ 28729*	*berkeleyensis*	Alameda Co.: Dwight Way Hill, Berkeley (37.8667885, -122.2420078)
X	X	MVZ 28770	*berkeleyensis*	Alameda Co.: Dwight Way Hill, Berkeley (37.8677891, -122.2367154)
X	X	MVZ 69963	*berkeleyensis*	Contra Costa Co.: 1 mi W summit Mount Diablo (37.881833, -121.9328333)
X	X	MVZ 69964	*berkeleyensis*	Contra Costa Co.: 1 mi W summit Mount Diablo (37.881833, -121.9328333)
X	X	MVZ 70238	*berkeleyensis*	Contra Costa Co.: 1 mi W summit Mount Diablo (37.881833, -121.9328333)
X	X	MVZ 70239	*berkeleyensis*	Contra Costa Co.: 1 mi W summit Mount Diablo (37.881833, -121.9328333)
X	X	MVZ 69961	*berkeleyensis*	Contra Costa Co.: W side Mount Diablo (37.8816953, -121.9130424)
X	X	MVZ 69962	*berkeleyensis*	Contra Costa Co.: W side Mount Diablo (37.8816953, -121.9130424)
X	X	MVZ 207393	*dixoni*	Mariposa Co.: 1.4 mi W Mt. Bullion (37.50331, -120.06969)
X	X	MVZ 207406	*dixoni*	Mariposa Co.: Hunter Valley Mt. (37.63996, -120.21697)
X	X	MVZ 207404	*dixoni*	Mariposa Co.: Hunter Valley Mt. (37.65594, -120.22132)
X	X	MVZ 207405	*dixoni*	Mariposa Co.: Hunter Valley Mt. (37.65594, -120.22132)
X	X	MVZ 21842	*dixoni*	Merced Co.: 1 mi N Snelling (37.52931, -120.4422)

Continued

Dorsal View	Ventral View	Museum Number	Subspecies Name	Locality (latitude, longitude)
X	X	MVZ 21848	*dixoni*	Merced Co.: 5 mi N Snelling (37.57188, -120.4247)
X	X	MVZ 33060	*dixoni*	Merced Co.: Delhi (37.43266, -120.777351)
X	X	MVZ 26805*	*dixoni*	Merced Co.: Delhi [near Merced River] (37.432086, -120.777169)
X	X	MVZ 207399	*dixoni*	Merced Co.: Kelsey Ranch, 5.2 mi E Snelling (37.54598, -120.35863)
X	-	MVZ 207400	*dixoni*	Merced Co.: Kelsey Ranch, 5.2 mi E Snelling (37.54598, -120.35863)
X	X	MVZ 207403	*dixoni*	Merced Co.: Kelsey Ranch, 5.2 mi E Snelling (37.54927, -120.34974)
X	X	MVZ 23613	*dixoni*	Stanislaus Co.: La Grange (37.6661, -120.469857)
X	X	MVZ 55059	*goldmani*	Fresno Co.: Warthan Creek, 4.5 mi SE Priest Valley (36.1576, -120.6097)
X	X	MVZ 29370	*goldmani*	Monterey Co.: 1 mi NE Seaside (36.620269, -121.822246)
X	X	MVZ 29130	*goldmani*	Monterey Co.: 1.25 mi S Soledad (36.407657, -121.319496)
X	X	MVZ 29113	*goldmani*	Monterey Co.: 2 mi E San Lucas (36.12973, -120.985298)
X	X	MVZ 195193	*goldmani*	Monterey Co.: 5.2 mi NE King City (36.270044, -121.06419)
X	X	LACM 88695	*goldmani*	Monterey Co.: 6.7 mi NE Soledad (36.4935, -121.23658)
X	X	MVZ 108314	*goldmani*	Monterey Co.: Camp Ord, 3.5 mi E Marina (36.664619, -121.74057)
X	-	MVZ 182332	*goldmani*	Monterey Co.: Dunes E bank Salinas River, 1.2 mi N and 2.1 mi E Greenfield (36.337722, -121.202646)
X	X	MVZ 182333	*goldmani*	Monterey Co.: Dunes E bank Salinas River, 1.2 mi N and 2.1 mi E Greenfield (36.337722, -121.202646)
X	X	MVZ 108323	*goldmani*	Monterey Co.: E side Salinas River, 5 mi W Salinas (36.677043, -121.736999)
X	X	MVZ 100851	*goldmani*	Monterey Co.: Gabilan Range, 5.5 mi ENE Soledad (36.458729, -121.234228)
X	X	MVZ 140086	*goldmani*	Monterey Co.: Hastings Natural History Reservation (36.37851365, -121.5568207)

Continued

Dorsal View	Ventral View	Museum Number	Subspecies Name	Locality (latitude, longitude)
X	X	LACM 1809	*goldmani*	Monterey Co.: King City (36.2119841, -121.1266009)
X	X	MVZ 108364	*goldmani*	Monterey Co.: Lewis Creek (36.2379, -120.9887)
X	X	MVZ 108342	*goldmani*	Monterey Co.: Mathews Ranch, Bitterwater Rd., 8 mi N King City (36.309584, -121.042606)
X	X	MVZ 100857	*goldmani*	Monterey Co.: Metz (36.356538, -121.207772)
X	X	MVZ 108316	*goldmani*	Monterey Co.: Monterey (36.59962, -121.897474)
X	X	LACM 1842	*goldmani*	Monterey Co.: Monterey, 7 mi NE (36.66538, -121.79696)
X	X	MVZ 108338	*goldmani*	Monterey Co.: mouth of Vaqueros Canyon (36.26527, -121.336082)
X	X	MVZ 108317	*goldmani*	Monterey Co.: Paraiso Springs, Sierra de Salinas (36.334091, -121.3701)
X	X	MVZ 29123	*goldmani*	Monterey Co.: San Lorenzo Creek, Peachtree Valley (36.133317, -120.747539)
X	X	MVZ 29104	*goldmani*	Monterey Co.: San Lucas (36.128617, -121.021368)
X	X	MVZ 3482	*goldmani*	Monterey Co.: Sandhills, 2 mi S mouth Salinas River (36.72202, -121.79811)
X	X	LACM 1845	*goldmani*	Monterey Co.: Salinas (36.6790917, -121.6426945)
X	-	MVZ 29360	*goldmani*	Monterey Co.: Seaside (36.60922, -121.835607)
X	X	LACM 7219	*goldmani*	Monterey Co.: Soledad, 2 mi S (36.39578, -121.3216)
X	X	MVZ 108327	*goldmani*	Monterey Co.: Stonewall Creek, 6.3 mi NE Soledad (36.4649, -121.304)
X	X	MVZ 108336	*goldmani*	Monterey Co.: Stonewall Creek, 6 mi N Soledad (36.454617, -121.220322)
X	X	MVZ 100844	*goldmani*	Monterey Co.: W side Arroyo Seco, 4 mi S Soledad (36.370979, -121.304004)
X	X	MVZ 108284	*goldmani*	Monterey Co.: W side Arroyo Seco, 4 mi S Soledad (36.374091, -121.328347)
X	X	MVZ 108322	*goldmani*	Monterey Co.: W side Salinas River, 5 mi W Salinas (36.67332, -121.74552)
X	X	MVZ 28506	*goldmani*	San Benito Co.: 1 mi N Cook Post Office, Bear Valley (36.547167, -121.1441667)

Continued

Dorsal View	Ventral View	Museum Number	Subspecies Name	Locality (latitude, longitude)
X	X	LACM 88717	*goldmani*	San Benito Co.: 2.2 mi S, 4.6 mi W Paicines (36.6972401, -121.3805177)
X	X	LACM 88720	*goldmani*	San Benito Co.: 2.3 mi S, 1.1 mi W Paicines (36.6965282, -121.2978362)
X	X	MVZ 122249	*goldmani*	San Benito Co.: 3 mi S and 1.25 mi E San Benito (36.467, -121.0585)
X	X	MVZ 123549	*goldmani*	San Benito Co.: 3 mi S and 1.25 mi E San Benito (36.467, -121.0585)
X	X	LACM 88719	*goldmani*	San Benito Co.: 4-1/2 mi S, 3 mi W Hollister, Fremont Peak Road (36.7905613, -121.4667115)
X	-	MVZ 195196	*goldmani*	San Benito Co.: 9.1 mi NE King City (36.282766, -120.987678)
X	X	LACM 32069	*goldmani*	San Benito Co.: Pinnicles National Monument, 1 mi W (36.5334228, -121.1629875)
X	X	MVZ 72675	*goldmani*	San Benito Co.: San Benito (36.5082208, -121.0816515)
X	X	MVZ 18402	*heermanni*	Amador Co.: 5 mi E Carbondale (38.40863, -120.91923)
X	X	MVZ 18408	*heermanni*	Amador Co.: 5 mi E Carbondale (38.40863, -120.91923)
X	X	MVZ 119035	*heermanni*	Amador Co.: Carbondale (38.41003, -121.013288)
X	X	MVZ 85254	*heermanni*	Calaveras Co.: 1.5 mi NW Sheepranch (38.2180278, -120.473572)
X	X	MVZ 84285	*heermanni*	El Dorado Co.: 7 mi W and 3 mi S Placerville (38.68622, -120.92705)
X	X	MVZ 31783	*heermanni*	Mariposa Co.: Dudley (37.75634, -120.11166)
X	X	MVZ 31790	*heermanni*	Mariposa Co.: Dudley (37.75634, -120.11166)
X	X	MVZ 108355	*jolonensis*	Monterey Co.: 5 mi S San Ardo, Salinas Valley (35.951118, -120.877877)
X	X	MVZ 190038	*jolonensis*	Monterey Co.: 5 mi W Jolon (35.972038, -121.263268)
X	X	MVZ 190039	*jolonensis*	Monterey Co.: 1.5 mi SW Jolon (35.946683, -121.176576)
X	-	MVZ 228908	*jolonensis*	Monterey Co.: Bayonet Course, Camp Roberts (35.803002, -120.744812)

Continued

Dorsal View	Ventral View	Museum Number	Subspecies Name	Locality (latitude, longitude)
X	X	LACM 3108	*jolonensis*	Monterey Co.: Hog Canyon (35.751993, -120.559204)
X	X	LACM 1823	*jolonensis*	Monterey Co.: Jolon (35.9708313, -121.1737985)
X	X	MVZ 29086	*jolonensis*	Monterey Co.: Jolon (35.97071, -121.173723)
X	X	MVZ 29087*	*jolonensis*	Monterey Co.: Jolon [Valley floor 1 mi SW Of] San Antonio River (35.970572, -121.176729)
X	X	MVZ 181316	*jolonensis*	San Luis Obispo Co.: 0.2 mi S Hwy. 1 and 0.3 mi W Railroad Tracks, Callender Substation, Nipomo Mesa (35.76924, -120.79965)
X	X	MVZ 29097	*jolonensis*	San Luis Obispo Co.: 2 mi S San Miguel (35.723588, -120.6973)
-	X	MVZ 106099	*jolonensis*	San Luis Obispo Co.: 2 mi NW Red Hills summit (35.617204, -120.277653)
X	X	MVZ 106100	*jolonensis*	San Luis Obispo Co.: 2 mi SE Bryson [Monterey Co.] T25S R8E S1 (35.76924, -120.79965)
X	X	MVZ 182343	*jolonensis*	San Luis Obispo Co.: 2.3 mi E and 4.9 mi S Shandon (35.581383, -120.327076)
X	X	MVZ 122134	*jolonensis*	San Luis Obispo Co.: 3.5 mi SE Cholame (35.695428, -120.252334)
X	X	MVZ 107520	*jolonensis*	San Luis Obispo Co.: 5 mi E and 4 mi S Shandon (35.59775, -120.28173)
X	X	MVZ 106098	*jolonensis*	San Luis Obispo Co.: Beartrap Creek, 1.5 mi W San Juan Creek (35.558351, -120.26144)
X	X	MVZ 100859	*jolonensis*	San Luis Obispo Co.: Indian Creek, 13 mi S Shandon (35.469437, -120.379015)
X	X	LACM 2951	*jolonensis*	San Luis Obispo Co.: Paso Robles, 5 mi W (35.63215, -120.77867)
X	X	MVZ 29061	*morroensis*	San Luis Obispo Co.: 4 mi S Morro (35.29653, -120.84369)
X	X	MVZ 29084	*morroensis*	San Luis Obispo Co.: 4.5 mi S Morro (35.28734, -120.84366)
X	X	MVZ 29060	*morroensis*	San Luis Obispo Co.: 4.5 mi S Morro (35.28734, -120.84366)
X	X	MVZ 29058	*morroensis*	San Luis Obispo Co.: 4.5 mi S Morro (35.28734, -120.84366)

Continued

Dorsal View	Ventral View	Museum Number	Subspecies Name	Locality (latitude, longitude)
X	-	MVZ 29059	*morroensis*	San Luis Obispo Co.: 4.5 mi S Morro (35.28734, -120.84366)
X	X	LACM 48464	*morroensis*	San Luis Obispo Co.: 7.2 mi SW Atascadero (35.41226, -120.75633)
X	X	LACM 1781	*morroensis*	San Luis Obispo Co.: Morro (35.3469077, -120.8486777)
X	X	LACM 32099	*morroensis*	San Luis Obispo Co.: Los Osos Valley; Corner Buckskin Rd & Los Osos Rd (35.30784, -120.8178748)
-	X	MVZ 51462	*swarthi*	Kern Co.: 2 mi E McKittrick (35.30459, -119.58658)
X	X	MVZ 57112	*swarthi*	Kern Co.: 10 mi NE Taft (35.243833, -119.3288333)
X	X	MVZ 16684	*swarthi*	Kern Co.: divide at 3000 ft, W of McKittrick (35.3055, -119.7461667)
X	-	MVZ 16688	*swarthi*	Kern Co.: divide at 3000 ft, W of McKittrick (35.3055, -119.7461667)
X	X	MVZ 16687	*swarthi*	Kern Co.: divide at 3000 ft, W of McKittrick (35.3055, -119.7461667)
X	X	LACM 88664	*swarthi*	Kern Co.: Maricopa, 1-1/2 mi S, 1/2 mi W; Hwy 166 (35.04, -119.42)
X	X	MVZ 14452	*swarthi*	Kern Co.: McKittrick (35.305667, -119.623)
X	X	MVZ 14455	*swarthi*	Kern Co.: McKittrick (35.305667, -119.623)
X	X	LACM 1049	*swarthi*	Kern Co.: Taft (35.1461198, -119.4559021)
X	X	MVZ 198627	*swarthi*	Kern Co.: Temblor Range summit on Hwy. 58 (35.35564, -119.82853)
X	X	MVZ 138344	*swarthi*	Monterey Co.: Metz, Salinas Valley (36.355297, -121.207773)
X	X	MVZ 196746	*swarthi*	San Luis Obispo Co.: 0.4 mi S Wells Ranch, Caliente Range (35.04427, -119.89468)
X	X	MVZ 181313	*swarthi*	San Luis Obispo Co.: 1.1 mi W and 0.5 mi N Temblor Peak (35.070583, -119.509332)
X	X	MVZ 181317	*swarthi*	San Luis Obispo Co.: 1.1 mi W and 0.5 mi N Temblor Peak (35.070583, -119.509332)

Continued

Dorsal View	Ventral View	Museum Number	Subspecies Name	Locality (latitude, longitude)
X	X	MVZ 107514	*swarthi*	San Luis Obispo Co.: 3.5 mi E and 0.5 mi N McChesney Mt. (35.285637, -120.17411)
X	X	LACM 48462	*swarthi*	San Luis Obispo Co.: 6 mi E Cuyama, Hwy 166 (34.9364747, -119.5085604)
X	X	MVZ 14438	*swarthi*	San Luis Obispo Co.: 7 mi SE Simmler, Carrizo Plains (35.27959, -119.89931)
X	X	MVZ 14440*	*swarthi*	San Luis Obispo Co.: 7 mi SE Simmler, Carrizo Plains (35.27959, -119.89931)
X	X	MVZ 196748	*swarthi*	San Luis Obispo Co.: 13.3 mi NW (by road) New Cuyama (35.04427, -119.89468)
X	X	MVZ 195959	*swarthi*	San Luis Obispo Co.: Beam Flat, Elkhorn Hills (35.0191166667, -119.4924833333)
X	X	MVZ 107505	*swarthi*	San Luis Obispo Co.: Camatta Creek (35.4464832, -120.2887243)
X	X	MVZ 159024	*swarthi*	San Luis Obispo Co.: Carrizo Plain, 3.8 mi S and 11.5 mi W Taft (Kern Co.) (35.07387, -119.66272)
X	X	MVZ 159026	*swarthi*	San Luis Obispo Co.: Carrizo Plain, 3.8 mi S and 11.5 mi W Taft (Kern Co.) (35.07387, -119.66272)
X	X	MVZ 159023	*swarthi*	San Luis Obispo Co.: Carrizo Plain, 7.5 mi E, 2.5 mi S Simmler (35.314796, -119.853567)
X	X	LACM 88770	*swarthi*	San Luis Obispo Co.: Carrizo Plains; 15 mi N Reyes Station, on Soda Lake Road (35.2213452, -119.8575801)
X	X	LACM 44899	*swarthi*	San Luis Obispo Co.: Carrizo Plain; Soda Lake Road, 8.5 mi N (35.2213452, -119.8575801)
X	X	LACM 33642	*swarthi*	San Luis Obispo Co.: Carrizo Plain (near rock formation) California Valley, 2 mi W (35.32507, -120.03753)
X	-	MVZ 224999	*swarthi*	San Luis Obispo Co.: Chimineas Ranch (35.0646848, -119.9309259)
-	X	MVZ 16683	*swarthi*	San Luis Obispo Co.: Cuyama Valley (35.113215, -120.09569)
X	-	MVZ 224683	*swarthi*	San Luis Obispo Co.: Elkhorn Plain Ecological Reserve (35.1253, -119.6362)

Continued

Dorsal View	Ventral View	Museum Number	Subspecies Name	Locality (latitude, longitude)
X	X	LACM 44900	*swarthi*	San Luis Obispo Co.: Hwy 166, 9 mi NW; Soda Lake Road (35.0435056, -119.5658314)
X	X	MVZ 224998	*swarthi*	San Luis Obispo Co.: Johnson Flat, Chimineas Ranch (35.0914451, -119.9685754)
X	-	LACM 32148	*swarthi*	San Luis Obispo Co.: La Panza Range; Pozo, 6 mi NE (35.36518, -120.3)
X	X	MVZ 46773	*swarthi*	San Luis Obispo Co.: La Panza Ranch, 11 mi W Simmler (35.384359, -120.167494)
X	X	LACM 44896	*swarthi*	San Luis Obispo Co.: Maricopa, 2 mi W (35.06078, -119.43621)
X	X	LACM 2397	*swarthi*	San Luis Obispo Co.: Painted Rock (35.1458615, -119.8606371)
X	X	LACM 2890	*swarthi*	San Luis Obispo Co.: Painted Rock (35.1458615, -119.8606371)
X	X	MVZ 125740	*swarthi*	San Luis Obispo Co.: Painted Rock, T32S R20E (35.146085, -119.860768)
X	X	MVZ 198632	*swarthi*	San Luis Obispo Co.: San Diego Creek, Temblor Range (35.33341, -119.84337)
X	X	MVZ 100862	*swarthi*	San Luis Obispo Co.: Santiago Springs, 1.5 mi S and 8 mi E Simmler (35.328304, -119.84525)
X	X	LACM 2398	*swarthi*	San Luis Obispo Co.: Simmler (35.3514558, -119.9859688)
X	X	LACM 52634	*swarthi*	San Luis Obispo Co.: Soda Lake (35.2437357, -119.8974605)
X	X	LACM 88739	*swarthi*	San Luis Obispo Co.: Taft, 14 WSW; Carrizo Plains, Hill Ranch (35.06512, -119.68415)
X	X	LACM 88780	*swarthi*	Santa Barbara Co.: 3.5 mi S, 11.5 mi W New Cuyama, Cottonwood Creek Canyon (34.9725188, -119.8843145)
X	X	LACM 88785	*swarthi*	Santa Barbara Co.: 9 mi N, 25 mi W New Cuyama (35.0784827, -120.1298346)
X	X	LACM 32076	*swarthi*	Santa Barbara Co.: Santa Maria, 19 mi NE; Cuyama Valley Gorge; Hyw 66, Sierra Madre Picnic Area (35.1087668, -120.0905112)

Continued

Dorsal View	Ventral View	Museum Number	Subspecies Name	Locality (latitude, longitude)
X	X	LACM 88795	*swarthi*	Ventura Co.: 25 mi W Gorman, 1/2 mi E Nettle Springs Camp (34.80362, -119.28258)
X	X	LACM 52640	*swarthi*	Ventura Co.: Ojai, S of Meyers Road, W of Oso Road (34.458687, -119.2881606)
X	X	MVZ 25172	*tularensis*	Fresno Co.: 1.25 mi S Dunlap (36.723617, -119.11036)
X	X	MVZ 122383	*tularensis*	Fresno Co.: 1.4 mi S and 10 mi E Mendota (36.7212, -120.1982)
X	-	MVZ 138342	*tularensis*	Fresno Co.: 3 mi N Mercey Hot Springs on Co. Rd. J1 (36.7317, -120.8804)
X	X	MVZ 143976	*tularensis*	Fresno Co.: 3.9 mi N Mercey Hot Springs on Co. Rd. J1 (36.7308, -120.8348)
X	X	MVZ 72723	*tularensis*	Fresno Co.: 6 mi E Panoche (36.5811, -120.6863)
X	X	MVZ 51461	*tularensis*	Fresno Co.: 7 mi E Coalinga (36.1364, -120.2236)
X	X	LACM 3106	*tularensis*	Fresno Co.: Coalinga (36.14, -120.359)
X	X	MVZ 25176	*tularensis*	Fresno Co.: Minkler (36.7166, -119.4641)
X	X	MVZ 43312	*tularensis*	Kern Co.: 1 mi N Pond (35.7316807, -119.3293466)
X	X	MVZ 66397	*tularensis*	Kern Co.: 1.75 mi SW Caliente (35.273, -118.6498333)
X	X	MVZ 44340	*tularensis*	Kern Co.: 2 mi NE Rose Station (34.9843933, -118.8900727)
X	X	MVZ 107498	*tularensis*	Kern Co.: 2 mi N McKittrick (35.3346666667, -119.623)
X	X	LACM 88678	*tularensis*	Kern Co.: 3.8 mi S, 2.2 mi E Arvin, on Comanche Point Road (35.14, -118.79)
X	X	LACM 88683	*tularensis*	Kern Co.: 7/10 mi S Grapevine; Grapevine Canyon, entrance of Mobil Oil Pump Station (34.9405943, -118.92983)
X	X	MVZ 183779	*tularensis*	Kern Co.: 7.5 mi S, 10.25 mi W Bakersfield (35.2130458, -119.2193935)
X	X	MVZ 14423	*tularensis*	Kern Co.: 8 mi NE Bakersfield (35.45038, -118.9092)
X	X	MVZ 107499	*tularensis*	Kern Co.: 8 mi W and 3 mi N McKittrick (35.349667, -119.765)

Continued

Dorsal View	Ventral View	Museum Number	Subspecies Name	Locality (latitude, longitude)
X	X	MVZ 28458	*tularensis*	Kern Co.: 20 mi S and 8 mi W Bakersfield (35.087333, -119.1485)
X	X	LACM 44902	*tularensis*	Kern Co.: Bakersfield off Hwy 58, 10 mi E; Towerline Road (35.3277214, -118.8065441)
-	X	LACM 52637	*tularensis*	Kern Co.: Buena Vista Lake, 5 mi N (35.3, -119.29)
X	X	MVZ 26806	*tularensis*	Kern Co.: Caliente Creek Wash (35.314667, -118.7855)
-	X	MVZ 26807	*tularensis*	Kern Co.: Caliente Creek Wash (35.314667, -118.7855)
X	X	MVZ 158793	*tularensis*	Kern Co.: Caliente Creek Wash, 8.3 mi E, 1.4 mi S Edison (35.326, -118.7256667)
X	X	MVZ 106095	*tularensis*	Kern Co.: Carneros Springs, Carneros Canyon (35.448, -119.846)
X	X	LACM 43947	*tularensis*	Kern Co.: Conners, .5 mi N, 1 mi E (35.19, -119.1)
X	X	MVZ 28462	*tularensis*	Kern Co.: mouth of Caliente Creek Wash (35.3146666667, -118.7855)
X	X	MVZ 47491	*tularensis*	Kern Co.: Rose Station (34.9627123, -118.9157426)
X	X	LACM 88658	*tularensis*	Kern Co.: San Joaquin Valley, 0.5 mi N, 1 mi E Conners (35.19, -119.1)
X	X	LACM 48479	*tularensis*	Kern Co.: Tehachapi, 13 mi SW (34.9948125, -118.2840382)
X	X	LACM 88690	*tularensis*	Kern Co.: Tejon Ranch House, 1.4 mi N, 2 mi E (35.05, -118.71)
X	X	MVZ 198289	*tularensis*	Kings Co.: ca. 12.6 mi SSE Avenal (35.83962, -120.01631)
X	X	MVZ 109124	*tularensis*	Madera Co.: ? mi E Madera on Yosemite Rd. (37.000122, -119.972192)
X	X	MVZ 109125	*tularensis*	Madera Co.: ca. 8 mi E Madera (37.010305, -119.931611)
X	X	MVZ 14386	*tularensis*	Merced Co.: Los Baños (37.060514, -120.84778)
X	X	MVZ 14390	*tularensis*	Merced Co.: Los Baños (37.060514, -120.84778)
X	X	MVZ 14404	*tularensis*	Madera Co.: Raymond (37.217068, -119.904732)

Continued

Dorsal View	Ventral View	Museum Number	Subspecies Name	Locality (latitude, longitude)
X	X	MVZ 116721	*tularensis*	Madera Co.: San Joaquin Experimental Range (37.090636, -119.721443)
X	X	MVZ 69952	*tularensis*	Merced Co.: Sweeney's Ranch, 22 mi WSW Los Baños (36.9037894, -121.0431988)
-	X	MVZ 14391	*tularensis*	Merced Co.: Sweeney's Ranch, 22 mi S Los Baños (36.7503089, -120.9217988)
X	X	MVZ 72756	*tularensis*	San Benito Co.: 1 mi S New Idria (36.4003658, -120.6742)
X	X	MVZ 72728	*tularensis*	San Benito Co.: 2 mi NNE New Idria (36.4443, -120.6724)
X	X	LACM 38154	*tularensis*	San Benito Co.: Panoche, 4 mi E; Panoche Creek (36.5922343, -120.7638276)
X	X	LACM 32064	*tularensis*	San Benito Co.: Panoche, 4 mi E; Panoche Creek (36.5922343, -120.7638276)
X	X	MVZ 100705	*tularensis*	San Benito Co.: Panoche Pass, 11 mi E Llanada (36, -120)
X	X	MVZ 72722	*tularensis*	San Benito Co.: Panoche Creek, 2 mi SE Panoche (36.57583, -120.80917)
X	-	MVZ 182319	*tularensis*	San Joaquin Co.: 12.5 mi S and 0.5 mi E Tracy (37.537437, -121.421432)
X	X	MVZ 143980	*tularensis*	San Joaquin Co.: Castle Rock, Corral Hollow (37.63995, -121.48969)
X	X	LACM 32119	*tularensis*	San Luis Obispo Co.: California City; Between Carrizo Plain & La Brea (35.1196166, -117.9652819)
X	X	MVZ 67168	*tularensis*	Stanislaus Co.: 10 mi W Gustine (37.246139, -121.19052)
X	X	MVZ 28488	*tularensis*	Tulare Co.: 2 mi W Earlimart (35.883447, -119.311289)
X	X	MVZ 89613	*tularensis*	Tulare Co.: 2 mi Up" Drum Valley Rd." (36.629584, -119.107569)
X	X	MVZ 14406	*tularensis*	Tulare Co.: Tipton (36.059519, -119.31074)

APPENDIX C

List of newly designed internal forward (F) and reverse (R) primers for cytochrome-b (*Cytb*) used for amplification and sequencing of ancient specimens of *Dipodomys heermanni*.

Strand	**Primer Name**	**Sequence (5'=3')**
F	CytbDheer11f	CCATCGTTGTCTAATTCAAC
R	CytbDheer192r	GTGTGTAATGTATAGCCAGGA
F	CytbDheer129f	GATGATGAAACTTCGGATCA
R	CytbDheer356r	GGTTTCTATATAAGAGTATGAGCC
F	CytbDheer304f	ATCACTTTTCTTCATCTGTCT
R	CytbDheer440r	ATATTTGTCCTCATGGCAG

APPENDIX D

Best models of evolution for cytochrome b (*Cytb*), NADH dehydrogenase 2 (*ND2*), and control region (*Dloop*) for each *Dipodomys heermanni* dataset as determined by jModelTest (Posada 2008) and PartitionFinder (Lanfear et al. 2012).

Data Set	**jModelTest**	**PartitionFinder**
Fresh tissue samples only		
Cytb		
1st codon position		K80+I
2nd codon position		JC
3rd codon position		HKY
ND2		
1st codon position		HKY
2nd codon position		F81+I
3rd codon position		HKY
Dloop	HKY+G	
Concatenated *Cytb, ND2*, and *Dloop*		
Cytb 1st and 2nd codon position		K80+I
ND2 and Cytb 3rd codon position		HKY+G
Dloop		HKY+I+G
ND2 1st codon position		HKY
ND2 2nd codon position		F81

Continued

Data Set	**jModelTest**	**PartitionFinder**
Fresh tissue and ancient samples		
Cytb		
1st codon position		K80+I
2nd codon position		JC
3rd codon position		HKY
Dloop	TPM1uf+G	
Concatenated *Cytb and Dloop*		
Cytb 1st and 2nd codon position		K80+I
Cytb 3rd codon position		HKY+G
Dloop		GTR+I+G

APPENDIX E

Uncorrected *p* distances within *Dipodomys heermanni*.

Data Set	Average	Minimum	Maximum
Fresh tissue samples only			
Cytb	1.23	0	3.14
ND2	1.07	0	3.59
Dloop	2.10	0	3.89
Fresh tissue and ancient samples			
Cytb	1.11	0	3.62
Dloop	2.45	0	6.11

APPENDIX F

Constrained (for each subspecies) and unconstrained Bayes tree scores for *Dipodomys heermanni*

Cytb Fresh and Ancient– Harmonic Mean
No constraint -1736.449
Subspecies Constrained:
D. h. arenae -1736.075
D. h. berkeleyensis -1774.206
D. h. dixoni -1738.279
D. h. goldmani -1783.852
D. h. heermanni -1744.444
D. h. jolonensis -1765.774
D. h. swarthi -1788.863
D. h. tularensis -1806.329

Cytb Fresh and Ancient – Arithmetic Mean
No constraint -1632.230
Subspecies Constrained:
D. h. arenae -1642.638
D. h. berkeleyensis -1663.342
D. h. dixoni -1642.446
D. h. goldmani -1694.493
D. h. heermanni -1654.273
D. h. jolonensis -1666.408
D. h. swarthi -1692.288
D. h. tularensis -1713.067

Dloop Fresh and Ancient – Harmonic Mean
No constraint -2628.056
Subspecies Constrained:
D. h. arenae -.637.129
D. h. berkeleyensis -2678.021
D. h. dixoni -2651.931
D. h. goldmani -2673.722
D. h. heermanni -2641.668
D. h. jolonensis -2683.227
D. h. morroensis -2635.064
D. h. swarthi -2664.976
D. h. tularensis -2725.181

Dloop Fresh and Ancient – Arithmetic Mean
No constraint -2526.771
Subspecies Constrained:
D. h. arenae -2553.487
D. h. berkeleyensis -2585.116
D. h. dixoni -2560.998
D. h. goldmani -2580.268
D. h. heermanni -2546.574
D. h. jolonensis -2595.899
D. h. morroensis -2537.969
D. h. swarthi -2571.065
D. h. tularensis -2619.036

APPENDIX G

Principal components of variance for *Dipodomys heermanni* morphology.

PC Axis	Standard Deviation	Proportion of Variation	Cumulative Proportion
Dorsal View			
PC1	0.1761	0.1898	0.1898
PC2	0.1659	0.1684	0.3582
PC3	0.1301	0.1036	0.4618
PC4	0.11071	0.07501	0.53678
PC5	0.10524	0.06777	0.60456
PC6	0.10115	0.06261	0.66716
PC7	0.09393	0.05399	0.72115
PC8	0.08638	0.04566	0.76681
PC9	0.08254	0.04169	0.80851
PC10	0.0719	0.03164	0.84014
PC11	0.07057	0.03047	0.87061
PC12	0.06616	0.02679	0.8974
PC13	0.06096	0.02274	0.92014
PC14	0.05544	0.01881	0.93895
PC15	0.04674	0.01337	0.95232
PC16	0.04491	0.01234	0.96466
PC17	0.03813	0.0089	0.97356
PC18	0.02987	0.00546	0.97902
PC19	0.02743	0.00461	0.98362
PC20	0.0215	0.00283	0.98645
PC21	0.01999	0.00244	0.98889
PC22	0.01633	0.00163	0.99052
PC23	0.01562	0.00149	0.99202
PC24	0.01458	0.0013	0.99332
PC25	0.0116	0.00082	0.99414
PC26	0.01014	0.00063	0.99477
PC27	0.009179	0.00052	0.99529
PC28	0.008608	0.00045	0.99574
PC29	0.008078	0.0004	0.99614
PC30	0.007913	0.00038	0.99652
PC31	0.007679	0.00036	0.99688

Continued

PC Axis	Standard Deviation	Proportion of Variation	Cumulative Proportion
PC32	0.007324	0.00033	0.99721
PC33	0.006846	0.00029	0.9975
PC34	0.00642	0.00025	0.99775
PC35	0.00611	0.00023	0.99798
PC36	0.005614	0.00019	0.99817
PC37	0.005137	0.00016	0.99833
PC38	0.004732	0.00014	0.99847
PC39	0.004433	0.00012	0.99859
PC40	0.004311	0.00011	0.9987
PC41	0.004003	0.0001	0.9988
PC42	0.003828	0.00009	0.99889
PC43	0.003768	0.00009	0.99898
PC44	0.003665	0.00008	0.99906
PC45	0.003181	0.00006	0.99912
PC46	0.003149	0.00006	0.99918
PC47	0.003131	0.00006	0.99924
PC48	0.002954	0.00005	0.9993
PC49	0.002837	0.00005	0.99935
PC50	0.002793	0.00005	0.99939
PC51	0.002692	0.00004	0.99944
PC52	0.002607	0.00004	0.99948
PC53	0.002568	0.00004	0.99952
PC54	0.002461	0.00004	0.99956
PC55	0.002336	0.00003	0.99959
PC56	0.002305	0.00003	0.99962
PC57	0.002142	0.00003	0.99965
PC58	0.002035	0.00003	0.99968
PC59	0.001938	0.00002	0.9997
PC60	0.001904	0.00002	0.99972
PC61	0.001875	0.00002	0.99974
PC62	0.001695	0.00002	0.99976
PC63	0.001635	0.00002	0.99978
PC64	0.001561	0.00001	0.99979
PC65	0.001436	0.00001	0.9998
PC66	0.00143	0.00001	0.99982
PC67	0.001402	0.00001	0.99983

Continued

PC Axis	Standard Deviation	Proportion of Variation	Cumulative Proportion
PC68	0.001366	0.00001	0.99984
PC69	0.001284	0.00001	0.99985
PC70	0.001252	0.00001	0.99986
PC71	0.001219	0.00001	0.99987
PC72	0.001202	0.00001	0.99988
PC73	0.001151	0.00001	0.99989
PC74	0.001078	0.00001	0.99989
PC75	0.001041	0.00001	0.9999
PC76	0.001013	0.00001	0.99991
PC77	0.0009849	0.00001	0.99991
PC78	0.0009435	0.00001	0.99992
PC79	0.0009399	0.00001	0.99992
PC80	0.0008818	0	0.99993
Ventral View			
PC1	0.1429	0.1783	0.1783
PC2	0.1247	0.1357	0.314
PC3	0.1229	0.132	0.446
PC4	0.1072	0.1004	0.5464
PC5	0.10285	0.09237	0.6388
PC6	0.07687	0.0516	0.6904
PC7	0.06883	0.04137	0.73177
PC8	0.06401	0.03578	0.76755
PC9	0.05892	0.03032	0.79786
PC10	0.05674	0.02812	0.82598
PC11	0.0534	0.0249	0.8509
PC12	0.0488	0.0208	0.8717
PC13	0.04761	0.0198	0.89147
PC14	0.04317	0.01627	0.90774
PC15	0.03831	0.01282	0.92056
PC16	0.03537	0.01093	0.93149
PC17	0.03147	0.00865	0.94013
PC18	0.03005	0.00788	0.94802
PC19	0.02816	0.00692	0.95494
PC20	0.02675	0.00625	0.96119
PC21	0.02513	0.00552	0.96671
PC22	0.02349	0.00482	0.97152

Continued

PC Axis	Standard Deviation	Proportion of Variation	Cumulative Proportion
PC23	0.0228	0.00454	0.97606
PC24	0.02029	0.00359	0.97966
PC25	0.01774	0.00275	0.98241
PC26	0.01716	0.00257	0.98498
PC27	0.01593	0.00222	0.9872
PC28	0.01429	0.00178	0.98898
PC29	0.01394	0.0017	0.99067
PC30	0.01081	0.00102	0.99169
PC31	0.01034	0.00093	0.99263
PC32	0.009847	0.00085	0.99348
PC33	0.009205	0.00074	0.99422
PC34	0.008366	0.00061	0.99483
PC35	0.007956	0.00055	0.99538
PC36	0.00747	0.00049	0.99587
PC37	0.007206	0.00045	0.99632
PC38	0.006802	0.0004	0.99672
PC39	0.006296	0.00035	0.99707
PC40	0.005821	0.0003	0.99737
PC41	0.005683	0.00028	0.99765
PC42	0.005299	0.00025	0.99789
PC43	0.004879	0.00021	0.9981
PC44	0.00451	0.00018	0.99828
PC45	0.004389	0.00017	0.99845
PC46	0.004141	0.00015	0.9986
PC47	0.003892	0.00013	0.99873
PC48	0.003786	0.00013	0.99885
PC49	0.003487	0.00011	0.99896
PC50	0.003302	0.0001	0.99906
PC51	0.00284	0.00007	0.99913
PC52	0.002683	0.00006	0.99919
PC53	0.002624	0.00006	0.99925
PC54	0.002569	0.00006	0.99931
PC55	0.002522	0.00006	0.99936
PC56	0.002387	0.00005	0.99941
PC57	0.002216	0.00004	0.99945
PC58	0.002062	0.00004	0.99949
PC59	0.002048	0.00004	0.99953

Continued

PC Axis	Standard Deviation	Proportion of Variation	Cumulative Proportion
PC60	0.001974	0.00003	0.99956
PC61	0.001882	0.00003	0.99959
PC62	0.001832	0.00003	0.99962
PC63	0.001774	0.00003	0.99965
PC64	0.001638	0.00002	0.99967
PC65	0.001596	0.00002	0.9997
PC66	0.001514	0.00002	0.99972
PC67	0.001477	0.00002	0.99973
PC68	0.001311	0.00002	0.99975
PC69	0.001305	0.00001	0.99976
PC70	0.001279	0.00001	0.99978
PC71	0.001245	0.00001	0.99979
PC72	0.001205	0.00001	0.99981
PC73	0.001155	0.00001	0.99982
PC74	0.001138	0.00001	0.99983
PC75	0.001085	0.00001	0.99984
PC76	0.001054	0.00001	0.99985
PC77	0.001028	0.00001	0.99986
PC78	0.001007	0.00001	0.99987
PC79	0.0009672	0.00001	0.99987
PC80	0.0009484	0.00001	0.99988
PC81	0.000932	0.00001	0.99989
PC82	0.0008831	0.00001	0.9999
PC83	0.0008523	0.00001	0.9999
PC84	0.0008357	0.00001	0.99991
PC85	0.0008154	0.00001	0.99991
PC86	0.0007864	0.00001	0.99992
PC87	0.0007532	0	0.99993
PC88	0.0007311	0	0.99993

APPENDIX H

Discriminant function analysis for *a priori* categories of subspecific designations and using the categories determined from the mclust results for both the ventral and dorsal view of *Dipodomys heermanni* morphological specimens.

Categories	**Prior Frequency**
Subspecies for dorsal view	
D. h. arenae	0.0493
D. h. berkeleyensis	0.069
D. h. dixoni	0.0591
D. h. goldmani	0.197
D. h. heermanni	0.0345
D. h. jolonensis	0.0837
D. h. morroensis	0.0394
D. h. swarthi	0.2266
D. h. tularensis	0.2414
Overall accuracy	0.2069
Subspecies for ventral view	
D. h. arenae	0.0459
D. h. berkeleyensis	0.0714
D. h. dixoni	0.0561
D. h. goldmani	0.1888
D. h. heermanni	0.0357
D. h. jolonensis	0.0867
D. h. morroensis	0.0357
D. h. swarthi	0.2245
D. h. tularensis	0.2551
Overall accuracy	0.2602
Mclust for dorsal view	
Cluster category 1	0.6305
Cluster category 2	0.0788
Cluster category 3	0.0739
Cluster category 4	0.2167
Overall accuracy	0.8867

Continued

Categories	Prior Frequency
Cluster category 1	0.3929
Cluster category 2	0.3367
Cluster category 3	0.1837
Cluster category 4	0.0867
Overall accuracy	0.8418